MINISTRY OF HIGHER EDUCATION AND SCIENTIFIC RESEARCH

REPUBLIC OF CÔTE D'IVOIRE
UNION - DISCIPLINE - TRAVAIL

UNIVERSITY
FELIX HOUPHOUET BOIGNY

TRAINING AND RESEARCH UNIT FOR STRUCTURE SCIENCES OF MATTER AND TECHNOLOGY

DEPARTMENT OF PROCESS METALLURGY AND METAL RECYCLING OF RWTH AACHEN UNIVERSITY

N°: 665

SPONSORED BY THE
Federal Ministry of Education and Research

MASTER

IN RENEWABLE ENERGY AND CLIMATE CHANGE

SPECIALITY: PRODUCTION AND TECHNOLOGY OF GREEN HYDROGEN

MASTER THESIS

Topic:

THE RECOVERY OF RARE EARTH METALS FROM BAUXITE RESIDUES

Presented in September, 2023, by:

KAMARA Mary Dora

JURY:

Dr. (MC) ZAHIRI Pascal	President	Associate Professor UFBH
Pr. ELLO Serge	Examinator	Professor UFBH
Dr. Bamba Adama	Main Supervisor	Assistant Professor UFBH
Dr.-Ing Srecko Stopic	Co-Supervisor	Privat Dozent IME RWTH

ACADEMIC YEAR: 2022-2023

DEDICATION

This work is dedicated to my father, the late Mr. Philip Yamba Kamara.

I love and miss you so much, Papa.

ACKNOWLEDGEMENTS

I would like to thank God for giving me strong from the start to the end of this Program, His loving kindness and tender mercies have kept me thus far. I want to thank my family for their never-ending support from the day I embarked on the Journey.

A big thank you to the funders and WASCAL for giving me this opportunity to be in the International master's Program in Energy and Green Hydrogen Technology.

To all directors of universities and institutions, I say thank you, for welcoming me fairly throughout the program without any form of bias.

Lecturers from all over the world that came teach us, thank you for your time, patience, words of encouragement, wise words and knowledge passed unto us all through the last two years.

To the Jury members thank you all for you time and a very big thank you goes to my main supervisor, Dr Adama Bamba, thank you for always being available for me, I appreciate you so much for always coming through for me.

Also, I am grateful to you Dr Srecko Stopic, for not just being an amazing and co-Supervisor to me, but for being my mentor, you have significantly supported not only on my thesis work but also making sure that my career path blossoms after this program. Your humble approach to research and science has been exceptionally inspiring, this approach has helped me tremendously and I will surely keep it with me throughout my career.

Thank you to all the 59 students in this first, I am grateful to have met all of you. In one way or the other, all of you have touched my life with your unique personalities, I say thank you.

Finally, I want to thank my family, and friends for their tireless support throughout this master program.

ABSTRACT

With the rising use of contemporary, environmentally friendly technology, there is an increase in the demand for crucial commodities like scandium and rare earth elements (REEs) and other valuable metals, which necessitates the use of innovative resources to secure supply. This thesis includes both pyrometallurgical and hydrometallurgical methods aiming decarbonizattion process for recovering valuable metals from bauxite residues, with the hydrogen plasma reduction and direct acid leaching serving as the primary approaches. The objectives of adopting these procedures are to provide alternative and/or creative techniques for the recovery of REEs and other valuable metals from materials like bauxite residue, which cannot be disposed of in an ecologically responsible manner following the Bayer chemical process, which extracts aluminum. As carbon smelting, which was previously used to recover REEs from BR, was inefficient due to using carbon as a reagent, hydrogen is now being investigated as a replacement. Hydrogen plasma reduction recovers about 99,9% of iron as crude metallic iron, which can be separated from slag that contains aluminum and silicon. In order to recover valuable metals like scandium and aluminum, the slag is treated or leached by acids. Bauxite residue is also subjected to direct acid leaching (hydrometallurgy) in order to extract rare earth elements such as yttrium, scandium. To obtain more effective and optimum outcomes, the pyrometallurgy and hydrometallurgy combination of the two techniques was also investigated. Effective characterisation techniques for examining the results of hydrogen plasma reduction and direct acid leaching studies for their mineralogical, chemical (macro component), and micro impurity investigations were described. The goal of extracting Fe, Al, Ti, and Si was accomplished since the data clearly indicate their presence and provide proof that they are vital for a sustainable future and all facets of human existence.

Key words : Bauxite residues, Aluminium, Pyro-hydrometallurgy, Acid , Rare earth elements**.**

RESUME

Avec l'utilisation croissante de technologies modernes et respectueuses de l'environnement, la demande de matières premières cruciales telles que le scandium et les éléments de terre rare (DER) et d'autres métaux précieux augmente, ce qui nécessite l'emploi de ressources innovantes pour assurer l'approvisionnement. Cette thèse comprend à la fois des méthodes pyrométallurgicales et hydrométallurgiques visant le processus de décarbonation pour la récupération des métaux précieux des résidus de bauxite, avec la réduction du plasma d'hydrogène et le déversement direct d'acide servant comme les approches primaires. Les objectifs de l'adoption de ces procédures sont de fournir des techniques alternatives et/ou créatives pour la récupération de REE et d'autres métaux précieux à partir de matériaux tels que les résidus de bauxite, qui ne peuvent pas être éliminés de manière écologiquement responsable à la suite du processus chimique Bayer, qui extrait l'aluminium. Comme la fonte du carbone, qui était auparavant utilisée pour récupérer les ERE de BR, était inefficace en raison de l'utilisation de carbone comme réactif, l'hydrogène est maintenant étudié comme substitut. La réduction plasmatique d'hydrogène recouvre environ 99,9% du fer en fer métallique brut, qui peut être séparé de la boue contenant de l'aluminium et du silicium. Pour récupérer des métaux précieux tels que le scandium et l'aluminium, la boue est traitée ou liquéfiée par des acides. Le résidu de bauxite est également soumis à un déversement direct d'acide (hydrométallurgie) afin d'extraire des éléments de terre rares tels que l'ytrium, le scandium. Pour obtenir des résultats plus efficaces et optimaux, la pyrométallurgie et la combinaison hydrométallurgique des deux techniques ont également été étudiées. Des techniques de caractérisation efficaces pour l'examen des résultats des études de réduction du plasma d'hydrogène et de fuite directe d'acide pour leurs recherches de mineralogie, de chimie (composant macro) et de microimpureté ont été décrites. L'objectif de l'extraction de Fe, Al, Ti et Si a été atteint puisque les données indiquent clairement leur présence et fournissent la preuve qu'elles sont vitales pour un avenir durable et toutes les facettes de l’existence humaine.

Mots clés : résidus de bauxite, aluminium, pyro-hydrométallurgie, acide, éléments de terres rares.

ACRONYMS AND ABBREVIATIONS

WASCAL : West African Science Service Center on Climate Change and Adapted Land Use

REE : Rare Earth Elements

BR : Bauxite Residues

RM : Red Mud

LED : Light Emitting Diode

USSG : United States Standard Gauge

ICP-OES : Inductively Coupled Plasma Optical Emission spectroscopy

XRD : X-Ray diffraction

EDX : Energy Dispersive X-Ray Analysis

EAF : Electric Arc Furnace

LED : Light-emitting diode

CD : Compact disc

ROM : Red only memory

DVD : Digital versatile disc

LIST OF TABLES

Table 1: Reduction of 20 g red mud to slag(first set of 5, 10, and 15 Mins Experiments) 27
Table 2: Reduction of red mud to slag(second set of 5, 10, and 15 Mins Experiments)... 27
Table 3 : Leaching of Slag with HCI, H_2SO_4 and NaOH 28
Table 4 : Direct leaching of 25g red mud with 250 ml acidic solution (HCI, & H_2SO_4) using 1mol/l and 200 rpm 29
Table 5: Operation data for XRD-Measurement 31
Table 6 : Dissolution of samples Results of BR/Slag & Metallic phase 32
Table 7 : Chemical Composition of BR from Zvornik 32
Table 8: Chemical Composition of Red Mud 34
Table 9 : Content of rare earth elements in BR, Zvornik 34
Table 10**:** X-ray diffraction analysis of red mud 36
Table 11: Comparative analysis of mineralogical phases of red mud after leaching 40
Table 12: Chemical composition of the obtained solution and calculated leaching efficiency 41
Table 13 : First set of hydrogen plasma reduction experience plus evaporates red mud .. 46
Table 14 : Secomd set of hydrogen plasma reduction experience plus evaporates red mud 46
Table 15 :First set of experiments for Metal (5 and 15 Minutes Reduction) 49
Table 16 : Second Set of experiments for metals (5, 10, and 15 Minutes Reduction) 50
Table 17 : Results for tungsten 50
Table 18 EDX macro components of Slag after leaching 51
Table 19 Comparative analysis of mineralogical phases of slag after leaching 52
Table 20 Results of micromixing (ICP-OES) 55
Table 21 : Leaching efficiency using values of content of oxides in slag and in solid residue after leaching of slag 56

LIST OF FIGURES

Figure 1: Bauxite (Sources/Usage : Public Domain Visit Media to see details) 8
Figure 2 : (Bauxite: structure of global reserves by region, https://marketpublishers.com/lists/23959/news.html 9
Figure 3 :Bauxite In Sierra Leone (https://vimetcobauxite.com/commencement-of-dry-beneficiated-bauxite/) 9
Figure 4: Diagram of Bayer Process(USSG, 2018) 10
Figure 5 :Bauxite residue deposit in Germany (https://de.wikipedia.org/wiki/Rotschlamm) 11
Figure 6 :An accent water pot made from lead **(**A bronze Kuei handled vessel on a rectangular plinth (34.30 x 44.50 cm) cast in China in the 7th century B.C. Courtesy of ©The Cleveland Museum of Art, Leonard C. Hanna, Jr. Fund, 1974.7) 12
Figure 7 : Metal and types of metals (https://byjus.com/jee/faq-alkaline-earth-metals-jee/) 13
Figure 8 :Metallurical Methods(Hydrometallurgy, Pyrometallurgically and Biohydrometallurgical processes) 15
Figure 9 :Ellingam diagram for carbon reduction 18
Figure 10 : Ellingam diagram for stability of metallic oxide 20
Figure 11 : The location of Bosnien (Mapdata @2023 GeoBasis-DE/BKG(@2009) 22
Figure 12: Red Mud from Bosnia 23
Figure 13 : Experimental set-up for the Hydrogen Plasma Reduction at the Max Planck Institut fuer Eisenforschung MPIE, and it is in Duesseldorf, Germany. 24
Figure 14 **(**Metallic-phase and Slag after Hydrogen Plasma Reduction**)** 24
Figure 15 : Iron/Metal after separation and Reduction 25
Figure 16 : Apparatus for direct Acidic leaching with Red Mud 25
Figure 17 : Experimental setup for the filtration (a) and drying processes of residue (b) 26
Figure 18:The area of accumulated Bauxite residue in Zvornik, Bosnia and Hercegowina. 33
Figure 19 : XRD-analysis of BR from Zvornik 35
Figure 20 : Redmud (15.05.2023) with 1 mol/L HCl, 90 °C, 120 min (Graphical representation) 37
Figure 21 : Redmud with 1 mol/L HCl, 90 °C, 120 min 37
Figure 22: Redmud 17.05,2023 with 1 mol/L H_2SO_4,90°C, 120 min (Graphical

representation) 38
Figure 23 Redmud 17.05,2023 with 1 mol/L H_2SO_4,90 °C, 120 min 39
Figure 24 : Compounds (X-axis)- leaching Efficiency (Y-axis) Leaching with 1M HCl (90°C, 2hours, s/L: 1/10) 42
Figure 25 : Compounds (X-axis)- leaching Efficiency (Y-axis) Leaching with 1M H2SO4 (90°C, 2hours, s/L: 1/10) 42
Figure 26*:Formation of silica gel after sulfuric acid leaching at 90°C* 43
Figure 27: Natural precipitation of iron after hydrochloric acid leaching at 90°C 43
Figure 28 : Graphical representation of Reduction of red mud to slag(first set of 5, 10, and 15 Mins Experiments) 44
Figure 29 : Graphical representation of Reduction of red mud to slag(first set of 5, 10, and 15 Mins Experiments) 45
Figure 30 : Metallic Phase 10 Mins after Reduction 46
Figure 31 : Composition of Slag, Metallic Phase and Evaporated Material Present in Percentage 48
Figure 32 : XRD Analysis of Fe, and $FeNi_{0.16}$. of metallic phase 49
Figure 33 : Leaching 2.5g slag with 1 mol H2SO4, 90°C, 120mins 53
Figure 34 : Leaching 2.5g slag, with 1 mol HCL , 90°C, 120 54
Figure 35 : HCl-Leaching 90°C, 2h (leaching efficiency (%)) 57
Figure 36 : H2SO4-Leaching 90°C, 2 h (leaching efficiency (%)) 58

Table of Contents

DEDICATION ..... *i*

ACKNOWLEDGEMENTS ..... *ii*

ABSTRACT ..... *iii*

RESUME ..... *iv*

ACRONYMS AND ABBREVIATIONS ..... **v**

LIST OF TABLES ..... *vi*

LIST OF FIGURES ..... *vii*

Introduction *1*

CHAPTER I: LITERATURE REVIEW *5*

1.1 THEMATICS **7**

1.1.1 Bauxite Ore **7**

1.1.2 General Overview on the Evolution of Metals 11

1.1.3 The Properties and Importance of Rare Earth Metals (Valuable Metals) 13

1.1.4 Pyrometallurgy and Hydrometallurgy 15

1.1.5 Carbon Reduction Process 17

1.1.6 Hydrogen Reduction Process 18

CHAPTER II: METHODS AND MATERIALS *21*

2.1. METHODS **21**

2.2. Materials And Study Area **21**

2.3. Instruments For The Hydrogen Plasma Reduction Experiments 23

2.4. Instruments For Direct Acidic/Base Leaching Experiments 25

2.5. FILTRATION AND DRYING PROCESSES **26**

2.6. Experiments **26**

2.7. Lists Of Experiments 27

2.8. Experiments For Hydrogen Plasma Reduction Of Red Mud To Slag 27

2.9. Lists Of Experiments Of Hydrogen Plasma Reduction Of Redmud to Slag and Leaching With HCL, H_2SO_4 & NaOH 28

2.10. LISTS Of EXPERIMENTS FOR DIRECT ACID LEACHING Of Red Mud 29

CHAPTER III: Results And Discussions *31*

3.1 Characterization Of Treated Sludge And Liquid Phase-Mineralogical And Chemical

Analysis **31**

3.2.HYDROMETALLURGICAL METHOD RESULTs **36**

3.3 PYROMETALLURGICAL METHOD RESULTs **44**

3.5 ICP OES analysis of metallic phase **49**

3.4 LEACHING OF THE OBTAINED SLAG AFTER PLASMA REDUCTION **51**

3.5 Chemical Analysis Of Micro Impurities (Icp-Oes Technique) **54**

CONCLUSION AND RECOMMENDATION ***58***

Bibliography **60**

INTRODUCTION

INTRODUCTION

Bauxite is a clay-like sediment that is the principal host for alumina. Generally, bauxite is a naturally occurring mineral, soil, or rock formation comprising a conglomerate of multiple aluminum-bearing minerals with other valuable impurities. Iron oxides (Fe_2O_3 and FeO(OH)), clay minerals, silica, kaolinite, titanium minerals, rutile, and anatase are among the contaminants. Bauxite is mined for aluminum production because of high concentrations of the following aluminum-bearing minerals:Gibbsite: $Al(OH)_3$, Boehmite: AlO(OH), and Diaspore: AlO(OH).

From an industrial perspective, bauxite is a material from which alumina is extracted using the Bayer Chemical Process (Gow & Lozej, 1993). A geological survey in 2020, shows the different continent where this natural resource is present all around the world, Africa constitutes (32%), Oceania (23%), South America and the Caribbean (21%), Asia (18%), and (6%) for the rest of the world. The bauxite resources present in the above-mentioned continents are estimated to be between 55 and 75 billion tons (USGS, 2020). Bauxite resources are distributed across countries as well. The countries with large amount of this reserve include Australia, Guinea, China, Brazil, India, Indonesia, Jamaica, Malaysia, Greece, Ghana, Guyana, Hungary, Romania, Sierra Leone, Suriname, Turkey, and Venezuela. Australia, Guinea, China, Brazil, and Jamaica are the top five countries with the highest bauxite reserves (Bogatyrev et al., 2009) (Gow & Lozej, 1993). Approximately 95% of aluminum extraction from bauxite is performed through the Bayer Chemical Process, and the process has been proven to be highly efficient. This process was named after its inventor, Karl Josef Bayer, an Austrian Chemist in 1888. Currently, it is known to be the most commonly used method for aluminum extrusion. This involves several steps, including Mining, Digestion, Clarification, Precipitation, and Calcination. In the Clarification step, the solid impurities precipitate, forming the Red Mud Sediment, and the liquid containing aluminum remains on top (Gow & Lozej, 1993)(Verma et al., 2017)(Balomenos et al., 2011).

Red Mud also known as bauxite residue, is generated during the clarification step of the Bayer Process. The process is based on contacting aluminium-bearing ores with a concentrated NaOH solution at temperatures between 150 – 250 ºC in an autoclave.

It is a reddish-brown sludge containing iron, titanium, and silicon oxides, the majority of aluminum oxides that were not extracted during the clarification step, and other valuable metals. It is a large aspect of aluminum production, and it is a highly alkaline residue, as

sodium hydroxide is added in the digestion step during the Bayer Process; each ton of processed alumina generates approximately 4-5 tons of red mud as a byproduct.

The mud normally produced is usually transported to a dam, where it undergoes a dehydration and drying process to reduce its volume and maintenance cost (Khairul et al., 2019) (Silveira et al., 2021a) (Archambo & Kawatra, 2021) (Borra et al., 2016) (Lemougna et al., 2017) (Ribeiro et al., 2012). The high alkalinity of bauxite residue (i.e. pH 10 – 13) is a main environmental concern. Moreover, spills have led to major environmental incidents, as it was the case of the Ajka disaster in Hungary in 2010 (Anton et al., 2014). In 2015, the collapse of a tailing dam in the state of Minas Gerais in Brazil evidenced as well the serious ecological and socio-economic impact of storing solid waste residue at large scale. Also, in Brazil, 10.6 million tons of red mud is thrown away per year, and the world produce about 117 million tons in the same year. (Mukiza et al., 2019).

The composition of the BR varies according to the type of bauxite, mining location, and process parameters of the Bayer Process. The chemical composition of BR contains 16% of alumina (Al_2O_3), 41.82 % of iron oxide (Fe_2O_3), 7.53% of silicon dioxide (SiO_2), 9.58% of titanium dioxide (TiO_2) and 3.29% of sodium oxide (Na_2O) as major constituents and 21% arsenic (As), chromium (Cr), copper (Cu), manganese (Mn), lead (Pb), and zinc(Zn), etc., as the minor constituents(Verma et al., 2017).

Rare earth elements are extracted together with the residue during the bayer process from the bauxite ore. REEs are typically enriched in the residue compared to when they are in bauxite due to two factors, which are: the quality of the ore, and the processing conditions employed. The recovery of REEs from bauxite residue is worthwhile, as they are currently considered censorious raw materials by many countries. The extraction of metals from bauxite residue is economically feasible and suitable extraction processes are available. Iron oxides are the main constituents of the bauxite residue, and they can make up to 60 % of the mass of the bauxite residue. The red color of the bauxite residue is caused by iron(III)oxides (mostly hematite and Fe_2O_3). The Rare earth elements are about fifteen metallic elements of the lanthanide series, including yttrium and scandium. These elements include: Lanthanum (La), cerium (Ce), praseodymium (Pr), neodymium (Nd), promethium (Pm), samarium (Sm), europium (Eu), gadolinium (Gd) , terbium (Tb), dysprosium (Dy), holmium (Ho), erbium (Er), thulium (Tm), ytterbium (Yb), lutetium (Lu), Scandium (Sc) and Yttrium (Y).

Since the beginning of alumina production, there has been a desire to utilize the bauxite residue produced by the Bayer process, either by recovering important metals from it or by employing it entirely in bulk applications. The most typical applications for bauxite residue are in the construction, industry, or agricultural industries as feedstock[(Ifg, n.d.)], as well as in the field of environmental protection through the neutralization and adsorption of hazardous elements from contaminated gas, water, and soil(Power et al., 2011). Despite the suggested application fields, there are incentives for better treatment techniques. For example, processing bauxite residue through recovery of major and minor metals to maximize the value provided and to minimize the residual solids produced each year.

Nowadays, industries have more focus towards sustainable manufacturing. Thus, the waste (Red Mud) from Bayer's process needs to be effectively utilized. The main problem with red mud is the considerable volume generated. Moreover, there is a huge hazard associated with water and soil contamination owing to their high alkalinity(pH between 10 and 13), the occurrence of heavy metals, and even traces of radioactive element. In addition to the need for large storage areas for disposal, permanent care is required for maintenance and monitoring. Brazilian companies spend approximately USD 106 million annually to ensure the safe disposal of red mud. Other impacts include air pollution from alumina refining in which caustic gases and other corrosive dust are released into the atmosphere. Vast amounts of water were fundamental throughout this phase of the process, although the most significant volume was reused(Silveira et al., 2021a). The above stated problems tells the world, researchers, and scientists that there is a lot of work to be done in this work. The effective and efficient extraction of valuable metals from this residue does not only help in protecting the environment and humanity from harmful diseases and gases, it also, helps in the industrialization sector. The problem is selective separation of iron during reduction in metallic phase, and dissolution of Y, Al, Ti from slag to liquid. Si stays in slag. The temperature, acid content, solid-liquid ratio, and leaching time are among the parameters that these studies examine. A combination of the characteristics of the raw materials and several technological factors affect how well the leaching process for recovering rare earth metals from bauxite residue works.

Leaching process efficiency can be greatly increased, leading to more effective and ecologically friendly recycling particles, by comprehending the interplay between these parameters and applying statistical analysis tools.

This work will focus on efficiently extracting four (Fe, Al, Ti, Si) out of about 20 elements from red mud as stated through the combination of pyrometallurgical and hydrometallurgical processes. Reduction efficiency and leaching efficiency/distribution of the four above listed elements are the main research questions, and they will be answered by the methods used in this work, these include: the hydrogen plasma reduction between slag and metallic phase (reduction) and liquid and solid residue (leaching with sulfuric acid and hydrochloric acid and NaOH). The main aim and objective of this work is to compare the influence time on the chemical composition of slag and metalic phase and also the reduction and leaching efficiency.

The work is divided into three chapters, the first one is based on the literature review followed by materials and methodology as second and then the third chapter is the results and discussion. A conclusion and some recommendations were made at the end.

CHAPTER I: LITERATURE REVIEW

CHAPTER I: LITERATURE REVIEW

For the several applications of this waste, it is essential to know the bauxite residue characteristics to highlight their potentialities. As discussed in the previous sections, BR is a waste resulting from the Bayer process for alumina production. Consequently, its constitution is a mixture of compounds initially present in the original ore (bauxite) and other substances generated during the Bayer cycle (Lyu et al., 2021).

Several studies revealed that the material contains aluminium hydroxides, alumina, iron oxides, quartz, titanium dioxide, calcium, and sodium oxides and hydroxides. In addition to these, other elements can be found in smaller quantities, namely Na, K, Cr, V, Ni, Ba, Cu, Mn, Pb, Zn and V, Ga, P, Mn, Mg, Zn, Th, Cr, Nb oxides (Silveira et al., 2021b) (Lima et al., 2017a). There is a variation in chemical composition among different red muds worldwide, as their composition is strongly influenced by the mineral deposit region (Filho et al., 2007). The oxides are organised in several minerals' forms, which also requires characterisation. (Hairi et al.) characterised the mineralogical composition of a red mud sample as containing hematite (Fe_2O_3), gibbsite (γ-$Al(OH)_3$), boehmite (γ-AlOOH), goethite (α-FeOOH), TiO_2 in the anatase polymorph, quartz (SiO_2), and a hydrated sodium alumi-nosilicate (1.08Na2O.Al2O3.1.68SiO2.1.8H2O) (Hairi et al., 2015). Hu et al. also detected quartz, hematite,calcite ($CaCO_3$), sodalite ($Na_8(Al_6Si_6O_{24})C_{l2}$),chantalite ($CaAl_2(SiO_4)(OH)_4$), and gibbsite in red mud (Hu et al., 2019). A similar Ukrainian study described red mud by the following mineralogical composition (% by mass): 25–27% hematite, 25–28% goethite, 4.5–6.5% rutile and anatase, 15–17% hydrogarnets, 6–7% sodium aluminosilicate hydrate, 2.5–3.0% calcite (Krivenko et al., 2017). Bădănoiu and her team found in their study hematite, iron titanium oxide, sodium aluminium silicate, aluminium silicate hydrate, cancrinite, and calcium aluminium silicate hydrate (Bədənoiu et al., 2015). There can also be organic compounds on the residue, as a result of vegetable and organic substances in the bauxite/overburden and modifiers or flocculants added during the process, mainly carbohydrates, alcohols, phenols, and the sodium salts of polybasic and hydroxy acids such as humic, fulvic, succinic, acetic, or oxalic acids (Zhang et al., 2020).

Red mud is extremely fine in terms of particle size distribution. According to Silva and other authors, 95% of the volume is below 44µm, with specific surface area (by Brunauer–Emmett–Teller (BET) analysis) values between 13 and 22 $m^2.g^{-1}$ (Filho et al., 2007). Sutar and other collaborators ((H Sutar et al., 2014)) described a distribution with

90% of the material with a particle size below 75 microns and a specific surface area between 10 and 30 $m^2.g^{-}1$. Lima and his teamdescribed specific surface area values in a larger range from 20 to 30 $m^2.g^{-1}$. In the same work, they characterised red mud with particles smaller than 290 µm and by its average diameter between 0.4 and 0.6 µm. The authors highlighted the importance of particle size measurement, as this strongly affects the rheological properties and, consequently, the possible applications for this material (Lima et al., 2017b). Likewise, Rai et al. identified red mud as extremely low in size, as its average diameter is smaller than 10 µm. They similarly referred to the specific surface area between 14 and 25 $m^2.g^{-1}$. Finally, according to this paper, red mud real density is around 3 to 3.8 g.cm−3 (Rai et al., 2020). The red mud's surface area may vary according to the type of manufacturing process and their methodologies. Shoppert et al. showed that the red mud's surface area from the Bayer process has a greater surface area than that obtained by the sintering process. However, when subjected to alkaline fusion at 300 ◦C, the surface area can double in size (Shoppert et al., 2019). The chemical characteristics, particle size distribution, and behaviour of the residue are affected by the original bauxite. In general, the coarse fraction (greater than 100 µm) is rich in quartz and can be separated from the finer silty muds (typically 80% less than 10 µm). These coarse fractions are known as "red oxide sand" or "sand residue", and only the fine portions are named "red mud". Usually, the first fraction is destined for road construction around the residue deposition locations as a drainage layer under the mud or as a topping material, as it has superior draining behaviour and inferior caustic behaviour (Danner, Tobias and Justnes, Harald, 2020). The red mud generated in Brazil has an average of 34% iron oxide and 5.5% titanium oxide, making it a potential source for these metals recovering. There is also the presence in low concentrations of rare earth elements, but its mineral phases are complicated to identify because they are associated with other oxides (Borra et al., 2015). According to Shinomiya, after the extraction, Fe2O3 can be used in steel metallurgy and TiO2 for paints and cosmetics production, and it also has potential for application in special alloys, suitable for prosthesis manufacturing and aerospace industry.

Ribeiro studied Brazilian red mud and found a specific surface area of 20.27 $m^2.g^{-1}$, density of 2.90 $g.cm^{-3}$, and a pH of 12.95. As expected, they also described alumina and iron oxide as the predominant red mud constituents, followed by smaller amounts of SiO_2 and Na_2O (or NaOH). As a result, the authors suggested that non-calcined red mud has the potential to be applied on mortars and concretes for non-structural applications,

partially replacing the cement in the mixture (D. V. Ribeiro et al., 2011). Mercury and other authors estimated red mud specific surface area as 12.96 $m^2.g^{-1}$ and density of 2.65 $g.cm^{-3}$. X-ray diffraction analysis in this paper detected hematite, goethite, gibbsite, sodalite, anatase, calcite, nepheline, perovskite, pseudo brookite, and quartz (Mercury et al., 2011). Romano et al. observed on their mineral characterisation sodalite because of bauxite digestion by caustic soda and the original ore minerals, hematite, quartz, goethite, calcite, anatase, and dicalcium silicate. They also found gibbsite from incomplete digestion (Romano et al., 2019). Alekseev and his team also described the mineral composition for red mud as hematite and quartz in the majority. However, they detected magnetite in their sample. The density of red mud was also different from the other studies mentioned. They found a much smaller value: 0.86 $g.cm^{-3}$ (Alekseev et al., 2019). Manfroi and her team detected chantalite, cancrinite, gibbsite, hematite, quartz, and calcite in the red mud. The particle size distribution showed that 100% of the particles were smaller than 18 μm (Manfroi et al., 2014).

In conclusion, red muds are a highly complex and diverse material. Therefore, the scientific community faces enormous challenges in standardising processes to develop a red mud recycle route.

1.1 THEMATICS

1.1.1 BAUXITE ORE

The word bauxite was derived from the French territory Les Baux. Bauxite is the parent of lateric rocks, which consist of aluminium hydroxide minerals such as boehmite (γ-AlO(OH)), diaspore (α-AlO(OH)) and gibbsite (γ-$Al(OH)_3$) (Verma et al., 2017). Bauxite is a major source of aluminum raw material. They represent a typical exogenous type of mineral resource formed due to theintense chemical weathering in hot and humid zones. Sedimentary products of the proximal redeposition of bauxites are always conjugated with their residual lateritic formations. Bauxites are also formed in the course of subaerial diagenesis. Bauxites formed on the karstified surface of limestones (karst bauxites) make up a separate genetic group. Deposits of different genetic groups are characterized by various forms of orebodies, localization conditions, structures, textures, and structures. The chemical composition of bauxites depends primarily on the composition of parental rocks, while the mineral composition depends on superimposed processes. At present, many hundreds (possibly thousands) of bauxite deposits are known, but the number of

large (reserve more than 100 Mt) and superlarge (reserve more than 250 Mt) deposits is only a few dozens. Bauxite are formed on the continental surface and controlled by several factors, among which the major ones are climatic, tectonic, petrochemical, petrophysical, geomorphological, hydrogeological, biogenic, and temporal features. Absence of even one of these factors rules out the possibility of this process (Bogatyrev et al., 2009).

Figure 1: Bauxite (Sources/Usage : Public Domain Visit Media *to see details)*

Rich aluminum rocks in subtropical and tropical regions lead to bauxite formation under the Earth's surface. As seen in Figure 1. red mud is reddish-brown in color, which indicates the presence of iron and alumina in bauxite.

Large deposits of bauxite are mostly found in Australia, Europe, Africa, Brazil, India, and Jamaica etc.

As shown in Figure 2 are the continents you can find large bauxite reserves. Africa happens be number in the figure above, second by South America & the Caribbean, followed by Oceania, Asia and the Rest of the World.

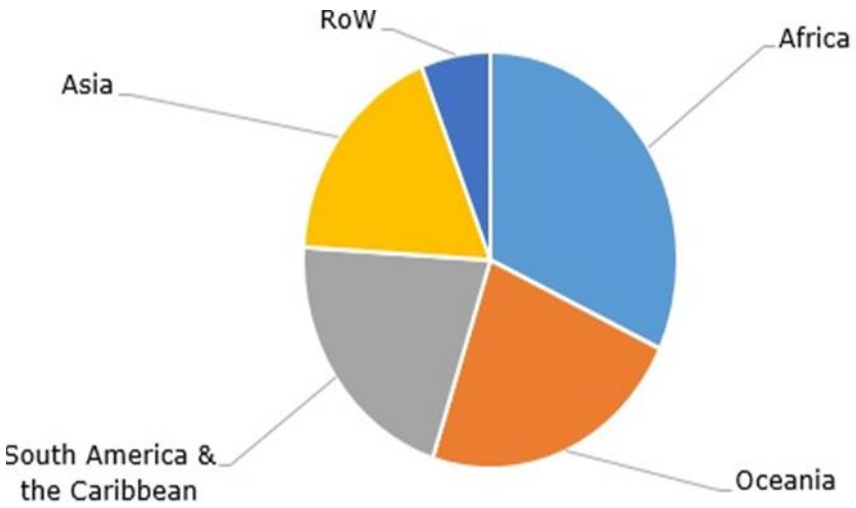

Figure 2 : (Bauxite: structure of global reserves by region, https://marketpublishers.com/lists/23959/news.html

Figure 3 :Bauxite In Sierra Leone (https://vimetcobauxite.com/commencement-of-dry-beneficiated-bauxite/)

The reserves are also distributed by country, the figure above show Bauxite mining activity in Sierra Leone were this reserve is found to be present. Figure 3 show the bauxite mining in Sierra Leone(Africa) one of the countries endowned with bauxite ore used for the aluminum extraction through the bayer chemical process. The figure displicts the miners in operation of mining bauxite ore in the mining site. This is a figure from one of the minning companies in Sierra Leone called Vimetco bauxite mining company located in the one of the provinces in Sierra Leone. A schematic diagram of the bayer chemical process is shown at figure 4.

DIAGRAM OF BAYER PROCESS

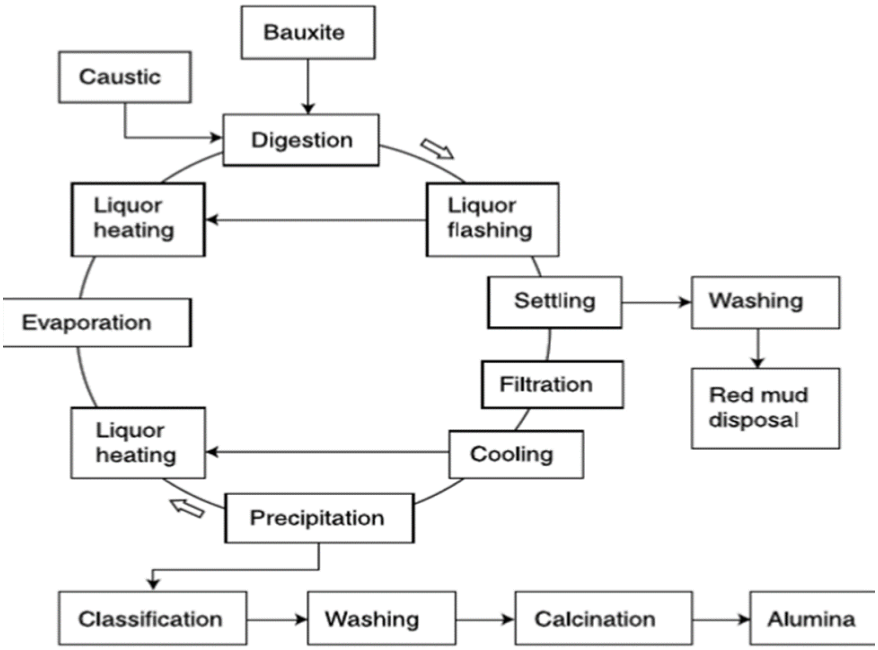

Figure 4: Diagram of Bayer Process(USSG, 2018)

Bauxite contains a high percentage of aluminum hydroxides and is, therefore, largely used to produce alumina (Al_2O_3) through the Bayer chemical process, which is based on the reaction with sodium hydroxide under heat and pressure. It also contains iron oxides, titanium dioxide, and other impurities as mentioned earlier.

Red mud, the waste of the Bayer Process, generally exits the process stream as a highly alkaline slurry (pH 10–12.5) with 15–30% solids and is pumped away for appropriate disposal. It is a complex material whose chemical and mineralogical composition varies widely depending on the source of bauxite and technological process parameters.

The Bayer process, named after its inventor Karl Bayer, is the most commonly used method for extracting aluminum from bauxite. This involves several steps, including mining, digestion, clarification, precipitation, and calcination.

The Bayer process is highly efficient in extracting aluminum from bauxite, and is used by most of the world's aluminum producers. The process involves several steps, which are: Digestion, Clarification, Precipitation, and Calcination.

Digestion: Finely ground bauxite ore is mixed with a sodium hydroxide solution (also known as caustic soda) under high temperature and pressure. This step dissolves aluminum compounds from the bauxite, leaving impurities behind.

Clarification: The resulting slurry is passed through a series of settling tanks to separate

the solid impurities from the liquid alumina-containing solution. The impurities settle as a red mud residue, while the clear liquid is called the pregnant liquor.

Precipitation: The pregnant liquor undergoes a series of steps to precipitate pure aluminum hydroxide. The addition of seed crystals promotes the growth of aluminum hydroxide particles.

Calcination: The aluminum hydroxide is heated in a rotary kiln or calciner to remove water and convert it into alumina.

The process generates a significant amount of red mud as a byproduct, which is stored in large containment areas and poses environmental challenges owing to its alkaline nature and potential for releasing contaminants into the surrounding ecosystem.

Efforts are being made to find sustainable uses for red mud, such as building materials and exacting valuable elements. Bauxite residue deposit in Germany is shown at Figure 5.

Figure 5 :Bauxite residue deposit in Germany (https://de.wikipedia.org/wiki/Rotschlamm)

The disposal of red mud has been kown to be a big challenge for the aluminium producing companies. The figure above shows the sludge stored in a sealed landfills until the hydroxides and silicates present as dispersions have settled. This is one of the largest red mud dumps in Germany, it is located near Stade in Lower Saxony between Butzflethermoor and Stadermoor, 10 km northwest of stade.

1.1.2 General Overview on the Evolution of Metals

Metal extraction and use are as old as humanity, having existed since the Stone Age. Native metals (Gold, Copper, and Silver) were discovered and used roughly 5000 years ago. They are a naturally occurring mineral and a subset of minerals, as they are

commonly referred to. Metals have played a crucial part in the growth of civilization and the evolution of people throughout history. Minerals were employed to make tools and weapons in ancient times, just as they are today. These metals were mined and used without all of the tools that are today employed for metal extraction, but over time, man tried to master how to identify, manipulate, and utilize these natural metals in more advanced ways and and in a variety of applications, allowing the development of human habitation. Pebbles and rocks, for example, for blunt implements, flint sticks and pieces for sparks, obsidian for knives, and so on. With the discovery of metals came the creation of bronze and iron, as well as the science of metallurgy, which revolves around the extraction of metals from their natural states, and the development of countries. Figure 6 depicts an antique water pot constructed of lead (which of metals) as another example of how versatile metals can be.

Figure 6 :An accent water pot made from lead (A bronze Kuei handled vessel on a rectangular plinth (34.30 x 44.50 cm) cast in China in the 7th century B.C. Courtesy of ©The Cleveland Museum of Art, Leonard C. Hanna, Jr. Fund, 1974.7)

It is clearly evident that the importance of metals in industrial revolution cannot be overrated, as the sudden increase in demand for metals in all spheres of life is alarming. It is needed both qualitatively and quantitatively in all works of life, hence the need for more researchers, and scientists to find more efficient and co-effective ways to recover all valuable metals from red mud also known as Bauxite Residue. As studies on the recovery of valuable metals keeps increasing as time progesses due to their importance in our society, it is also a good way of stopping the environmental damages and effects that are accompanied by bauxite residues because of its high alkalinity level.

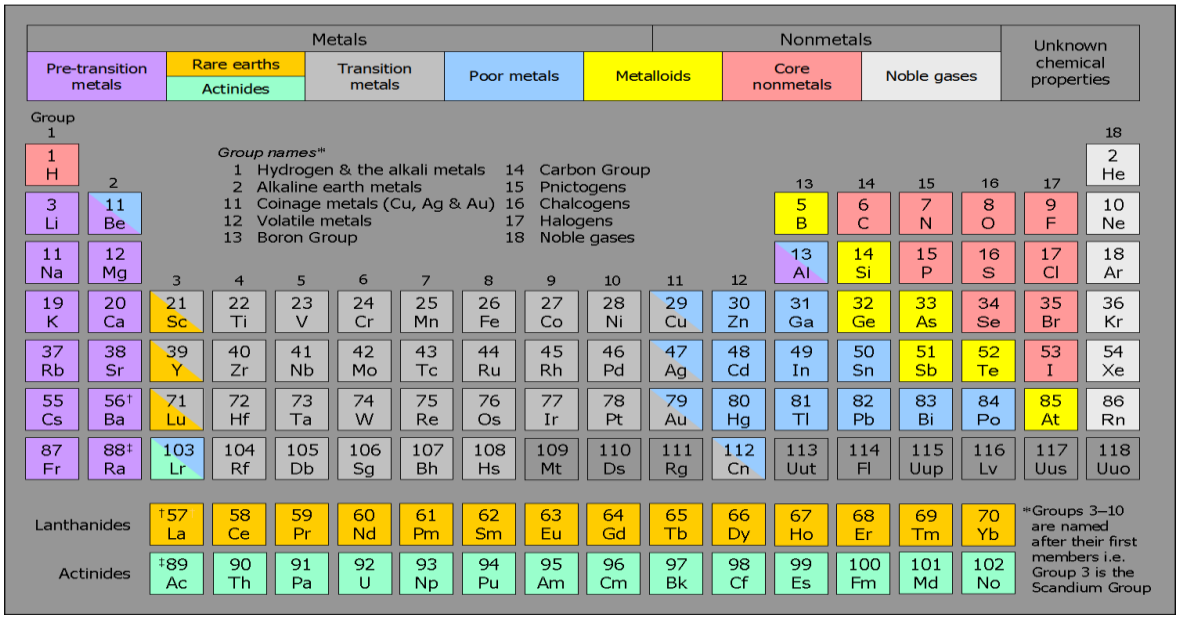

Figure 7 : Metal and types of metals (https://byjus.com/jee/faq-alkaline-earth-metals-jee/)

Figure 7, shows the different type of metals in the periodic table. Starting from Hydrogen and the alkali metals to the Lanthanides. Lanthanides, often known as rare earth elements, are the metals that run from Cerium (Ce) to Lutetium (Lu) on the top extended row of the periodic table. The third row's twenty first and thirty-ninth metals are the other rare earth metals. These are Yttrium and Scandium. They display the same chemical characteristics as other lanthanides. Though fewer lanthanides occasionally exhibit distinct valencies, rare earth metals are mostly trivalent in nature. Tetravalent elements include, for instance, cerium, praseodymium, and terbium. Samarium, europium, and ytterbium, on the other hand, are divalent elements.

1.1.3 The Properties and Importance of Rare Earth Metals (Valuable Metals)

There are around 17 soft heavy metals that are rare earth elements. These are also frequently referred to as precious metals or rare earth metals. Although Scandium and Yttrium are also regarded as rare earth metals since they are found in the same ore deposits as lanthanides and have comparable chemical characteristics, these metals are distributed across the periodic table as lanthanides. However, compared to lanthanides or rare earth metals, Scandium and Yttrium have different magnetic and electrical properties. All of these rare earth minerals share 25% of uses because of their comparable chemical properties, but 75% of their uses are due to their distinctive qualities. Even while rare

earth elements have similar chemical qualities, they differ greatly in terms of their physical characteristics due to their unique electrical and magnetic properties. For instance, the melting temperature of lutetium, the final rare earth element in the series, is substantially higher than that of lanthanum, the prototype of the lanthanide series, which has a melting point of 9180C or 16840F. It has been determined that lutetium has a melting point of 16630C or 30250F. Other groups of elements do not have such extreme variations in physical attributes. For instance, the difference in the melting points of copper, silver, and gold is just 1000C.

Rare earth metals naturally occur together in minerals, they share common properties with each other and therefore it id difficult to separate or distinguish them most times. They have high electrical conductivity and there is very little difference in the solubility and complex formation ability of the rare earth metals. Rare earth metals are found with non-metals in their third oxidation state (3+). There is very little tendency of these metals to exhibit different oxidation states. An exception to this is Europium a with valency(2+) and Cerium with a valency of 4+.

Due to their unusual physical and chemical properties, such as unique magnetic and optical properties, REEs have diverse applications that touch many aspects of modern life and culture. Specific REEs are used individually or in combination to make phosphors—substances that emit luminescence—for many types of ray tubes and flat panel displays, in screens that range in size from smart phone displays to stadium scoreboards. Some REEs are used in fluorescent and LED lighting. Yttrium, europium, and terbium phosphors are the red-green-blue phosphors used in many light bulbs, panels, and televisions. The glass industry is the largest consumer of REE raw materials, using them for glass polishing and as additives that provide color and special optical properties. Lanthanum makes up as much as 50 percent of digital camera lenses, including cell phone cameras. Lanthanum-based catalysts are used to refine petroleum. Cerium-based catalysts are used in automotive catalytic converters. Magnets that employ REEs are rapidly growing in application. Neodymium-iron-boron magnets are the strongest magnets known, useful when space and weight are limiting factors. Rare-earth magnets are used in computer hard disks and CD–ROM and DVD disk drives. The spindle of a disk drive attains high stability in its spinning motion when driven by a rare-earth magnet. These magnets are also used in a variety of conventional automotive subsystems, such as power steering, electric windows, power seats, and audio speakers. Nickel-metal hydride

batteries are built with lanthanumbased alloys as anodes. These battery types, when used in hybrid electric cars, contain significant amounts of lanthanum, requiring as much as 10 to 15 kilograms per electric vehicle. Cerium, lanthanum, neodymium, and praseodymium, commonly in the form of a mixed oxide known as mischmetal, are used in steel making to remove impurities and in the production of special alloys.

1.1.4 Pyrometallurgy and Hydrometallurgy

There are two possible processes so far that are been used for the recovery of valuable metals from bauxite residue. Namely: Pyrometallurgy and Hydrometallurgy. This can be done by either using the Hydrometallurical process on its own or combine both the pyrometallurgical and hydrometallurgical processes (Wang et al., 2011).

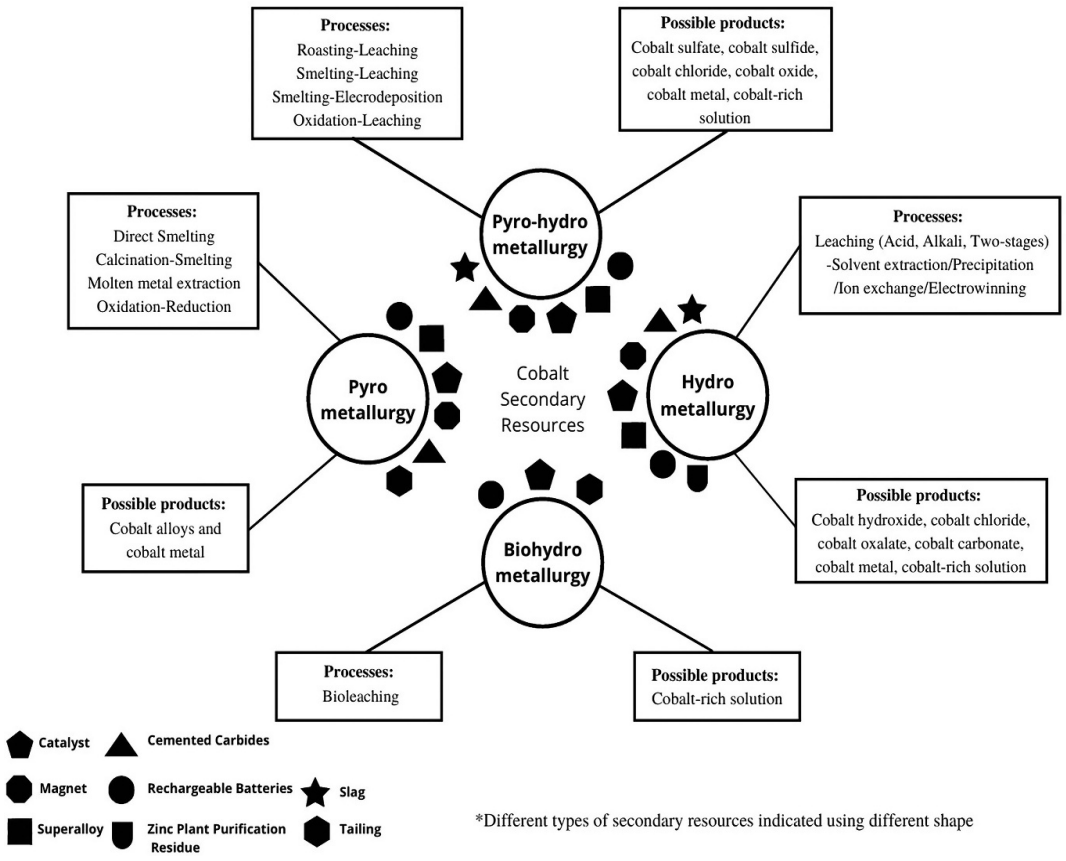

Figure 8 :Metallurical Methods(Hydrometallurgy, Pyrometallurgically and Biohydrometallurgical processes)

Hydrometallurgy is a branch of extractive metallurgy that deals with the processes of separating and recovering metals from their ores or other metal-bearing materials using aqueous solutions. In hydrometallurgical processes, the metal is typically dissolved into a liquid please(often acidic or alkaline solution) from the solid ore or raw material, and then various chemical and physical methods are employed to separate and purify the desired metal from the solution(Wang et al., 2011).

Red mud, also known as bauxite residue, is a byproduct generated during the extraction of alumina from bauxite ore using the Bayer process. It is a mixture of various compounds, including iron oxides, silicon dioxide, titanium dioxide, and other impurities, and is highly alkaline due to the use of sodiu hydroxide in the Bayer process. In addition to these components, red mud also contains valuable metals, such as rare earth elements (REEs). Acidic leaching of red mud is a specific hydrometallurgical process used for the recovery of rare earth metals from red mud. The process involves treating the red mud with an acidic solution, typically sulfuric acid or hydrochloric acid. The acidic environment dissolves the rare earth metals, as well as other valuable metals present in the red mud, into the leaching solution, leaving behind the non-leachable residues. The recovery of rare earth metals from red mud through acidic leaching is of significant interest due to the growing demand for these elements in various modern technologies, such as electronics, renewable energy, and other high-tech applications. Furthermore, it provides an opportunity to reduce environmental concerns related to the disposal of red mud, as it can convert a waste product into a valuable resource(Anton et al., 2014). However, it's essential to address the environmental impact and sustainability of these processes and find ways to optimize the extraction efficiency while minimizing the consumption of chemicals and energy.

Pyrometallurgy is another branch of extractive metallurgy that involves high-temperature processes to extract and refine metals from their ores or metal-containing materials. In contrast to hydrometallurgy, which uses aqueous solutions, pyrometallurgy relies on the application of heat and various chemical reactions to achieve metal extraction and purification. In the context of red mud and the recovery of rare earth metals, pyrometallurgy is not directly related to acidic leaching. Acidic leaching, as explained earlier, involves the use of aqueous solutions and is a hydrometallurgical process. However, pyrometallurgy might be utilized in some other stages of rare earth metal

recovery or in processing types of ores(Wang et al., 2011). One common application of pyrometallurgy in the context of rare earth metals is in the initial processing of rare earth ores. Before subjecting the ores to hydrometallurgical methods like acidic leaching, they may undergo roasting or smelting, which are pyrometallurgical processes. Roasting involves heating the ores in the presence of oxygen to remove volatile components and to convert certain compounds into more soluble forms that can be subsequently leached. Smelting, on the other hand, involves the use of high temperatures to melt the ores and separate valuable metals from gangue minerals. The combination of pyrometallurgical and hydrometallurgical processes is often used to optimize the recovery of rare earth metals from various sources. For example, after roasting or smelting the rare earth ores to prepare them for leaching, acidic leaching may be employed to dissolve the rare earth metals and separate them from other elements. This integrated approach allows for the efficient recovery of rare earth metals from complex ores or materials like red mud(Power et al., 2011; Wang et al., 2011).

1.1.5 Carbon Reduction Process

A carbon reduction process is a method used for the extraction of metals from their oxide ores. In this process, carbon acts as a reducing agent by combining with the oxygen present in the metal oxide, resulting in the formation of carbon dioxide (CO2) or carbon monoxide (CO). The process is employed for metals that are less electropositive and more reactive than carbon. The basic principle of the carbon reduction process involves heating the metal ore with carbon, such as coke or carbon monoxide, in order to remove oxygen from the metal oxide and obtain the metal in its elemental form. The reduction reaction can be represented as follows:

Metal oxide+Carbon→Metal+CO or CO2

It is important to note that this method works effectively for metals that are less reactive, typically those placed below aluminum in the reactivity series. For example, metals like iron (Fe), zinc (Zn), lead (Pb), and copper (Cu) can be extracted using the carbon reduction process. On the other hand, highly reactive metals like sodium (Na) cannot be extracted using carbon reduction, and other methods such as electrolysis are used for such cases. See figure 9 below for more information.

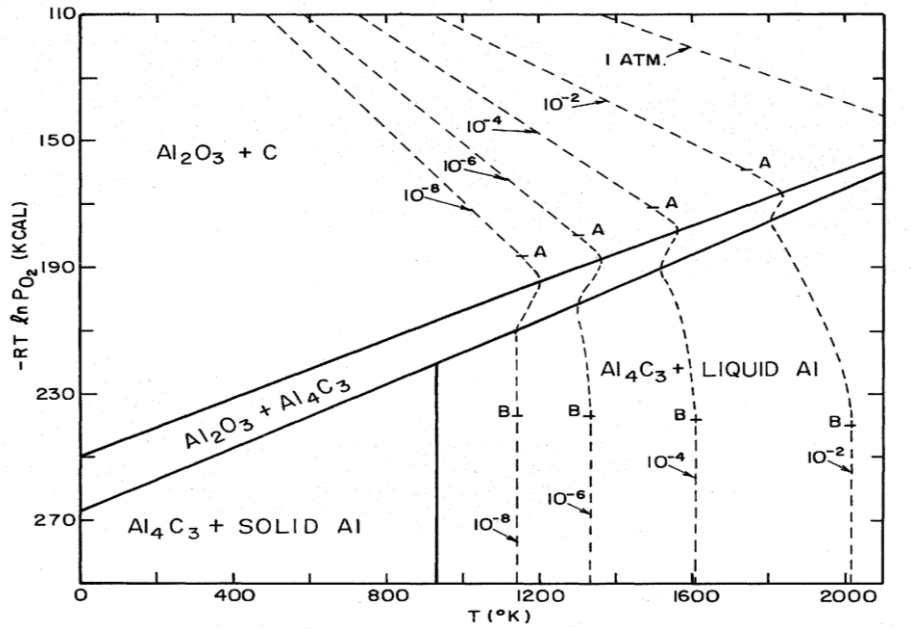

Figure 9 :Ellingam diagram for carbon reduction

1.1.6 Hydrogen Reduction Process

The harmless gas hydrogen is flammable at a wide range of concentrations and is colorless, odorless, tasteless, and flammable. Specific characteristics of hydrogen, such as its flammability and explosivity, include some of the following: Over a wide range of concentrations, hydrogen is flammable. Hydrogen has a very low ignition energy, and is flammable at atmospheric pressure at concentrations of between 4% and 74.2% by volume. Under bright light, the flame from burning hydrogen can be indistinct (Stopić & Friedrich, 2023).

Hydrogen reduction refers to a process in which hydrogen gas (H_2) is utilized as a reducing agent to convert metal oxides into their respective metals or other desired products. This process involves the reaction of hydrogen gas with metal oxides, resulting in the removal of oxygen from the oxide and the formation of water vapor (H_2O) as a byproduct instead of carbon dioxide(CO_2), which is typically produced when carbon-based reductants are used. The hydrogen reduction process has a significant implications for various industries, particularly in metallurgy, where it is employed as an alternative method for reducing iron ore to produce metallic iron without the need for a liquid phase. Conventional iron and steel production, particularly in blast furnaces, relies on coke as both an energy source and reducing agent, generating considerable amounts of CO and CO_2 in the process. By replacing coke with hydrogen gas, the hydrogen reduction process allows for the reduction of carbon dioxide emissions, making it a more environmentally friendly steelmaking process. The kinetics of the reduction process play a crucial role in

determining process productivity and efficiency. Researchers and industries are exploring ways to optimize the hydrogen reduction process by investigating parameters that influence and limit the reaction kinetics to achieve higher efficiency and operate close to the thermodynamic limit(Spreitzer & Schenk, 2019).

Ellingham diagram of metal oxides including the hydrogen (red color), hydrogen plasma (green color) , and carbon lines is shown at Figure .The Gibbs free energy change for a metal oxide reduced by molecular hydrogen into its lower oxide and its metal is shown below.

$MOx + H_2(g) \rightarrow MOx_{-1} + H_2O(g)$…….. Equation 1

$\Delta G = \Delta G^o + RT \ln (pH_2O/pH_2)$……..Equation 2

In this case, no signifcant contribution of ΔS to ΔG due to small entropy change from $H_2(g)$ to $H_2O(g)$.

Hydrogen is only commercially utilized in a limited number of refractory metals (i.e., W, Mo) and partly utilized in Ni and Co metals production. Hydrogen reduction of metal oxides has been extensively studied at laboratory scale, particularly in regard to kinetics and reaction mechanism. As shown at Figure 10 the reduction of iron oxides is highly possible with carbon and hydrogen in comparison to aluminium oxide and titanium oxide. Hydrogen is a weaker reductant compared to carbon at high temperatures, and the endothermic nature of hydrogen reduction of oxides means that the whole energy balance in existing reactors need to be revisited.

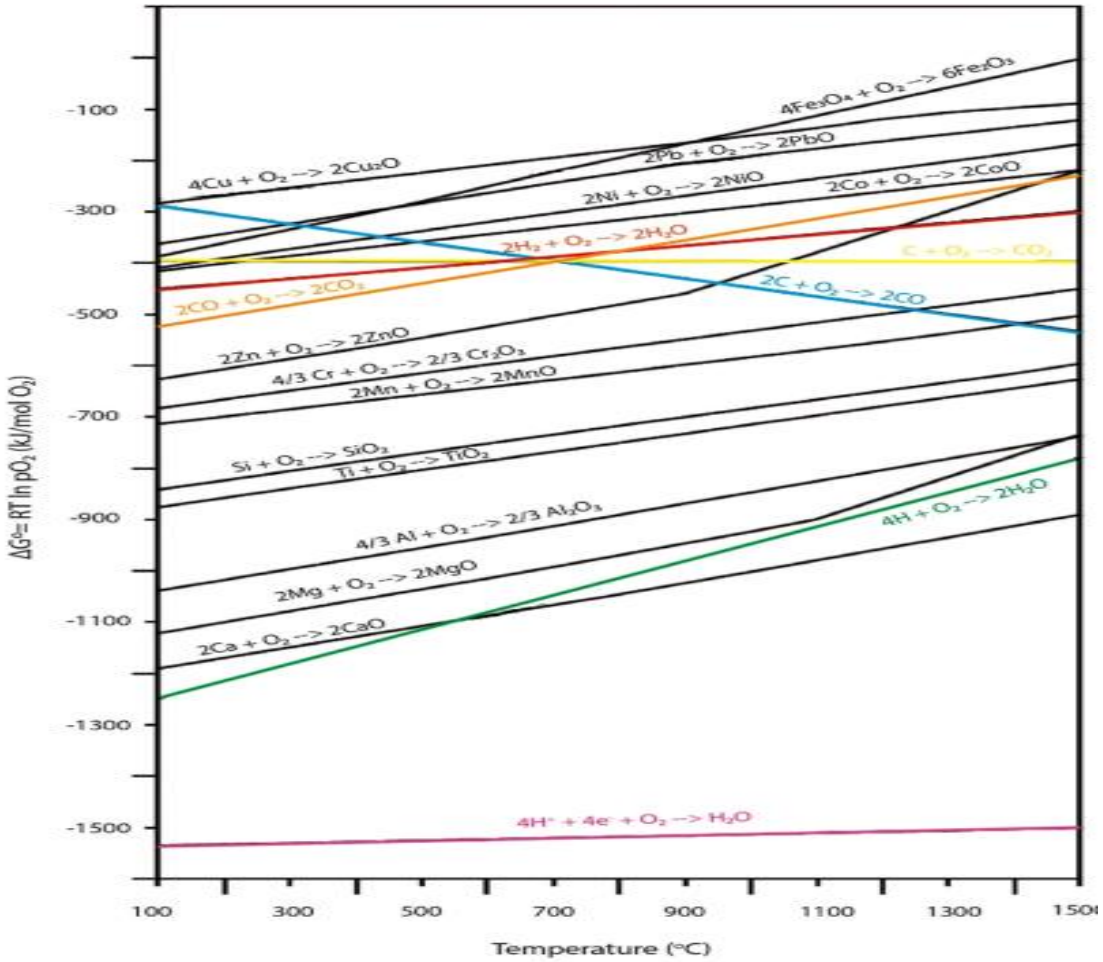

Figure 10 : Ellingam diagram for stability of metallic oxide

The current paper reviews by Rukini et al. *(REf. A. Rukini, M.A. Rhamdani, A van den Bulck, Metals production and metals oxxides reduction using hydrogen : A review, Journal of Sustainable Metallurgy (2022) 8:1–24 https://doi.org/10.1007/s40831-021-00486-5;* selected key studies and provides information on the current status and applications of hydrogen for reduction of metal oxides (with a focus on reduction kinetics and mechanisms of non-ferrous oxides). This study summarized that hydrogen has the potential to be used to recover valuable metal from secondary resources (e.g., Zn from EAF dust, Pb from slag) but further detailed fundamental studies are required for improved.

CHAPTER II : METHODS AND MATERIALS

CHAPTER II: METHODS AND MATERIALS

2.1. METHODS

In the previous chapter of this work, we dilated on the background of the study, the problem statement, the hypothesis, and objectives of the study. Here, we will deliberate on the research methodology which involves techniques that were used in the research process to collect, analyze, and evaluate the data in this study. We will also see detailed explanation about how all the main work was done, from the origin of the main material used, to the laboratory instrument set-up for experiments, and different processes of these experiments. Both hydrometallurgical and pyrometallurgical methods were used for treatment of bauxite residues.

In this study our results of hydrometallurgical treatment of bauxite residue from ALUMINA Zvornik using sulfuric acid and hydrochloric acid will be shown in order to study the change of mineralogical composition and pyrometallurgical treatment of the same bauxite residue. This residue will be reduced using hydrogen plasma reduction process in an electric arc furnace which aims to know the mineralogical and chemical composition of reducing red mud to get a Metallic Iron Phase and Slag. It also aims at knowing the chemical composition of slag and the metallic phase using ICP-OES, XRD, and EDX . Leaching efficiency will be calculated using ICP OES analysis, also XRD-Analysis will be used for the characterization of initial material and solid residues studying the change of mineralogical phases.

Mineralogical characterization of samples was carried out using X-ray diffraction technique – XRD. After the measurement, we processed the spectral images of the sample with the help of Difrac software. EVA v 4.2.2. The obtained values d (2θ), which are characteristic for each mineralogical phase, were compared with the literature data in the existing database, and thus we identified the present crystal phases.

2.2. MATERIALS AND STUDY AREA

The Bauxite residue used in this work was from Bosnia-Herzegovina, abbreviated as BiH, and in short often known informally as Bosnia. It is a country in Southeastern Europe as shown in Figure 12, located on the Balkan Peninsula, Sarajevo is the capital and largest city. Bordered by Croatia to the north, west and south, Serbia to the east, and Montenegro to the southeast, Bosnia and Herzegovina are almost landlocked, except for 20 kilometers (12 miles) of coastline on the Adriatic Sea surrounding the city of Neum. In the central and eastern interior of the country the geography is mountainous, in the northwest it is

moderately hilly, and the northeast is predominantly flatland. The inland is a geographically larger region and has a moderate continental climate, bookended by hot summers and cold and snowy winters. It is located at Lat 43° 54' 59.54" N and Long 17° 40' 19.74" E, with a population of about 4,590,000 people. Alumina d. o. o. Zvornik is the company where the bauxite residue used in the project was gotten from. It is located in the industrial zone of Zvornik, at the republic of Srpska, Bosnia, ang Herzegovina. The Alumina Factory was released into operation on 6th October 1978 and in the period 1984 - 1989 has paid a special attention to a development of products in the area of alumosilicate chemistry. During that period five plants were built, which beside raw material resources, are also using Alumina factory's infrastructure. It is the only company on the West Balkan and south part of the Middle Europe which is processing bauxite by **Bayer's process** and producing different types of hydrates and alumina. The mines around this vicinity supplies the bauxite to this Alumina company after production in advantages of it having a good quality(micro impurity and organics content). This company exports to a lot of countries because of the quality of alumina they produce, these countries include: Spain, France, Italy, Germany, Denmark, Netherland, Switzerland, Austria, Slovenia, Slovakia, Macedonia, Hungary, Czech Republic, Romania, Bulgaria, Poland, Ukraine, Russia, Belarus, Croatia, Serbia, Montenegro, Greece, Turkey, Israel, Saudi Arabia, Jordan, Tunis, Egypt, Sudan, Morroco, Algeria, Pakistan, India, China, USA, Columbia, and Costa Rica. Geographical map of bosnia and herzegowina is shown at Figure 12

Figure 11 : The location of Bosnien (Mapdata @2023 GeoBasis-DE/BKG(@2009)

Red mud, alumina zvornik, Bosnia und Herzegovina after washing and drying is shown at 13.

Figure 12: Red Mud from Bosnia

Figure 13, shows the red mud used for this work, and it was taken from a Alumina Factory in Zvornik, Bosnia. This bauxite residue consist 49.29 Fe_2O_3, 10.52 SiO_2, 12.03.Al_2O_3; 4.59 TiO_2, 8.23 CaO, 1.45 Na_2O), after washing and drying as shown in table 12. It was used in all the experiments i.e hydrogen plasma reduction and direct acid leaching experiments. The total amount of the main oxide phases amasses to about 85 wt.%, is it safe to assume that the remaining weight is mostly a result of remaining water and clay material.

2.3. Instruments For The Hydrogen Plasma Reduction Experiments

Solid-state reduction of bauxite residue in an electric Arc furnace hydrogen plasma has been proposed as an innovative technology to separate iron from bauxite residue.

a) Electric Arc Furnace

b) Formiergas

Figure 13 : Experimental set-up for the Hydrogen Plasma Reduction at the Max Planck Institut fuer Eisenforschung MPIE, and it is in Duesseldorf, Germany.

Figure 14 (a & b), shows an **electric arc furnace** (**EAF**) and separation of Metallic Plase & Slag. It is a furnace that heats material by means of an electric arc. Industrial arc furnaces range in size from small units of approximately one-tonne capacity (used in foundries for producing cast iron products) up to about 400-tonne units used for secondary steelmaking. Arc furnaces used in research laboratories and by dentists may have a capacity of only a few dozen grams. Industrial electric arc furnace temperatures can reach 1,800 °C (3,300 °F), while laboratory units can exceed 3,000 °C (5,400 °F). In electric arc furnaces, the charged material (the material entered into the furnace for heating, not to be confused with electric charge) is directly exposed to an electric arc, and the current from the furnace terminals passes through the charged material.

The Electric Arc Furnace used for hudrogen reduction operated under the following parameters: 20g of Red mud(BR), Total preesure was 900bar, Current was 200A, Gas was Argon 10%H2, and a temperature of 2500°C.

Slag After Hydrogen Reduction

a) Metallic-phase & Slag together b) Separation of Metallic Plase & Slag

Figure 14 (Metallic-phase and Slag after Hydrogen Plasma Reduction)

After plasma hydrogen reduction is done with the electric arc furnace shown in figure 14a and b, to reduce the bauxite reside into slag and a metallic phase, Figure 14a shows a clear picture of how the reddish brown bauxite residue looks like after the reduction process. Figure 14b is where separation of slag and metallic phase, as the residue after reduction is hidden by an hammer and thus the metallic phase leaves the slag. Both slag and metallic phase are separated and measure separately for analysis, in order to know all

the possible elements/metals present in both slag and metallic phase.

a) Metallic- Phase after separation b) Metallic-Phase after 15mins red.

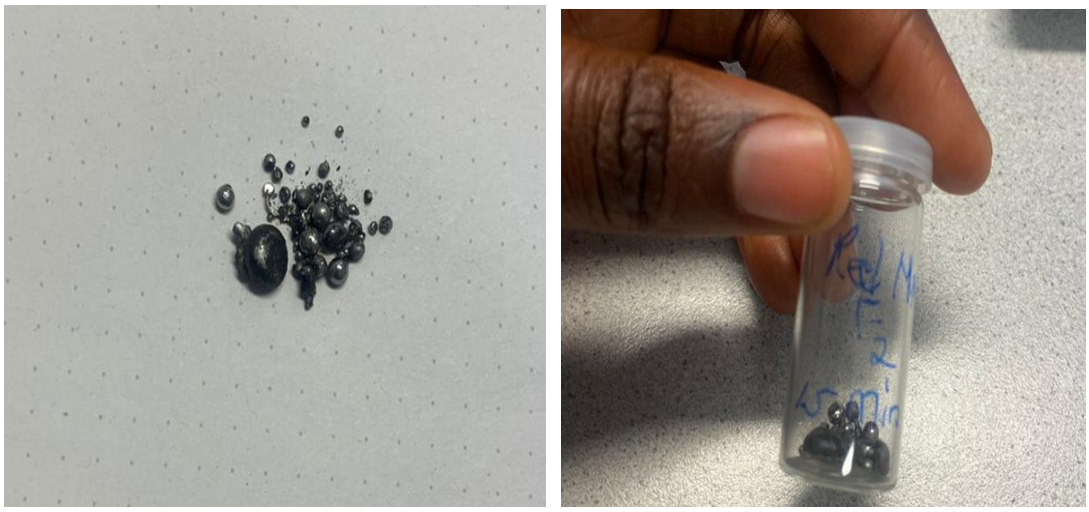

Figure 15 : Iron/Metal after separation and Reduction

Figure 15 (a & b) shows the metallic phase of bauxite residue after hydrogen plasma reduction process. The bauxite residue shown above was reduce for 15 mins in a electric arc furnace with different parameters.

2.4. Instruments For Direct Acidic/Base Leaching Experiments

Dissolution experiments were performed in small leaching equipment shown at Figure 16.

a) Before Leaching b) During Leaching

Figure 16 : Apparatus for direct Acidic leaching with Red Mud

This is a experimental setup for acidic leaching process of red mud. Figure 16 a & b give a clear view of how the aparatus for direct acidic before and during leaching is done. In figure 16a, an empty vacuum glass with sub-parameters are clearly seen, while in 16b, acid(HCl/H_2SO4) has been added to the vacuum glass under a specific time, red mud will be added to the acid and leaching will take place for a period of either 30/60/90/120 minutes, as per the aim of the experiment.

2.5. FILTRATION AND DRYING PROCESSES

Filtration was important in order to seprate the produced leaching solution from solid residue, as shown at Figure 17. Drying was performe in drying mashine, as shown at Figure 17.

a) Instrument for filtration after leaching b) Drying instrument of residue after filtration

Figure 17 : Experimental setup for the filtration (a) and drying processes of residue (b)

In figure 17a, a fitration machine is seen. This machine is used to filter the solid residue from the liquid residue after leaching. It works with a filter papper, place during filtration. Figure 17b, is used for drying the solid residue after direct leaching with acids.

2.6. EXPERIMENTS

The experiments for this work were done in two laboratories, the pyrometallurgy aspect (hydrogen plasma reduction) experiments were done at Max Planck Institut fuer Eisenforschung MPIE, Duesseldorf, Germany while the hydrometallurgically aspect (acidic leaching) experiments were done at the Metallurgical Process Technology and Metal Recycling(IME) at RWTH Aachen University. In order to characterize the samples,

the following were performed: XRD mineralogical analysis, chemical analysis of macrocomponents (EDX technique) and chemical analysis of micro impurities (ICP-OES technique) in the chemical laboratory of company ALUMINA; Zvornik, Bosnia and Herzegowina.

2.7. Lists Of Experiments

The experiments where done in two different ways based on the metallurgical processes involved, namely: Pyrometallurgy (Hydrogen Plasma Reduction) and Hydrometallurgy (Acidic Leaching). Different experiments were conducted for both Hydrogen Plasma Reduction and Acidic Leaching.

2.8. Experiments For Hydrogen Plasma Reduction Of Red Mud To Slag

Table 1 and 2 gives an information about the sets of hydrogen plasma reduction experiments done for 5, 10, and 15 mins. 20g red mud was initially added to the electric arc furnace, the tables also give information about the total mass after reduction, mass of iron metal, and mass of slag for each time interval as shown in Tables 2 and 3 respectively.

Table 1: Reduction of 20 g red mud to slag(first set of 5, 10, and 15 Mins Experiments)

NO	REDUCTION TIME (Mins)	TOTAL MASS AFTER REDUCTION (g)	MASS OF IRON METAL (g)	MASS OF SLAG (g)
1	5	13.02	1.300	11.725
2	10	10.681	2.848	7.833
3	15	8.839	2.239	6.600

Table 2: Reduction of red mud to slag(second set of 5, 10, and 15 Mins Experiments)

NO	REDUCTION TIME (Mins)	TOTAL MASS AFTER REDUCTION (g)	MASS OF IRON METAL (g)	MASS OF SLAG (g)
1	5	12.420	1.700	10.720
2	10	12.270	2.620	9.650
3	15	11.402	1.982	9.420

The tables displays the experiments that were done using the hydrogen plasma reduction process. In this process, the pyrometallurgical method was involved, as 20g of red mud (bauxite residue) was added into a furnace red mud to slag and acid or base leaching with total pressure of 900bar, current of 200A, Temperature of 2500°C and Gas that was around 10% H_2. The reduction process was done by several batches due to the inability of the furnace to take the material Red Mud in large scale. The maximum capacity of the furnace was 30g but because of work reliability and for the furnace to produce efficient results, we decided to use 20g as the maximum capacity for the three different reduction experiments done. The experiments in the furnace were also done in different time intervals as one of the aims of the work is to investigate the chemical compositions of red mud after reduction in different time intervals. The reduction was done for 5, 10 and 15 Minutes respectively, with 20g initial mass of red mud

2.9. Lists Of Experiments Of Hydrogen Plasma Reduction Of Redmud to Slag and Leaching With HCL, H_2SO_4 & NaOH

Table 3 : Leaching of Slag with HCI, H_2SO_4 and NaOH

No	STIRRING SPEED (Per Minute)	SLAG(g)	RED. TIME (Mins)	LEACHING AGENTS (Millilitres)	TIME (Mins)	TEMP (°C)
1	200	2.5	15	50 HCL	120	60
2	200	2.5	10	50 HCL	60	60
3	200	2.5	15	50 H2SO4	120	60
4	200	2.5	10	50 H2SO4	60	60
5	200	2.5	5	50 H2SO4	120	90
6	200	2.5	10	50 H2SO4	120	90
7	200	2.5	15	50 H2SO4	120	90
8	200	2.5	5	50 NaOH	120	90
9	200	2.5	10	50 NaOH	120	90
10	200	2.5	15	50 NaOH	120	90

Table 4, shows all the direct leaching with slag obtained after hydrogen plasma reduction process. The leaching reagents includes: Hydrochloric acid(HCL), sulfuric acid(H_2SO_4) and Sodium hydroxide (NaOH). The experiments were done with the 5, 10, & 15 mins slag leached with the reagents and different leaching time and temperatures.

Table 5, shows all 24 experiments of direct acidic leaching with red mud. Hydrochloric acids (HCL) and Sulfuric acids (H_2SO_4) were used during these experiments, with different temperatures, time intervals, solid/liquid ratios e.t.c. as shown in the table above.

2.10. LISTS Of EXPERIMENTS FOR DIRECT ACID LEACHING Of Red Mud

Table 4 : Direct leaching of 25g red mud with 250 ml acidic solution (HCI, & H_2SO_4) using 1mol/l and 200 rpm

NO	**ACIDS (1 mol)**	**TEMP. (°C)**	**TIME (Mins)**
1	H_2SO_4	90	120
2	H_2SO_4	90	90
3	H_2SO_4	90	60
4	H_2SO_4	90	30
5	H_2SO_4	70	120
6	H_2SO_4	70	90
7	H_2SO_4	70	60
8	H_2SO_4	70	30
9	H_2SO_4	50	120
10	H_2SO_4	50	90
11	H_2SO_4	50	60
12	H_2SO_4	50	30
13	HCL	90	120
14	HCL	90	90
15	HCL	90	60
16	HCL	90	30
17	HCL	70	120

18	HCL	70	90
19	HCL	70	60
20	HCL	70	30
21	HCL	50	120
22	HCL	50	90
23	HCL	50	60
24	HCL	50	30

CHAPTER III : RESULTS AND DISCUSSIONS

CHAPTER III: RESULTS AND DISCUSSIONS

The aim of the work is to efficiently extract and/or recover valuable and rare earth metals from bauxite residue which is a by-product of the bayer aluminum process. The characterization of the different chemical compositions/components presents in the bauxite residue after experimental work will be discussed here. Results for the mineralogical analysis(XRD), chemical analysis of macrocomponents (EDX) and chemical analysis of micro impurities (ICP-OES) will be discussed in detail with graphical and tabular representations in this chapter

3.1 CHARACTERIZATION OF TREATED SLUDGE AND LIQUID PHASE-MINERALOGICAL AND CHEMICAL ANALYSIS

Sample preparation was performed in single steps. The samples needed to be prepared so that their granulation was about 50μm, so that a flat-surface pallet could be made in polyethylene molds. In most samples, it was difficult to fulfill this condition due to the hardness of the samples that could not be prepared in the crucible. Regardless of the difficulties, it was managed to make a pallet that did not have a flat surface. The operational conditions are present in Table 6.

Table 5: Operation data for XRD-Measurement

Device	Model	Producer	Current	Voltage	Time per step	Range 2θ	step
XRD	Endeavor D8	Bruker	40mA	35KV	40mA	10-90	0.5

To determine the elements in ppm-range, samples are measured on the ICP-OES device, using an optical emission technique that uses inductive-coupled plasma as a source. This technique is intended for analysis trace elements and requires translating the sample into an acidic solution. Sample preparation was performed using method - ISO 6607-1985. The method involves the destruction of the sample with three concentrated acids (sulfuric, nitric and hydrochloric) at the beginning, and the treatment of the precipitate with hydrofluoric acid to translate residual elements (except SiO_2) into solution. After this preparation, a complete dissolution was expected. Total dissolution was confirmed during treatment of solid residue obtained in leaching experiments at 90°C as shown in table

Table 6 : Dissolution of samples Results of BR/Slag & Metallic phase

Designation of the Sample	Dissolution of Samples(%)
Mud 15.05.2023.	100
Mud 17.05.2023.	100
Slag 10min HCl	95.4
Slag 15min HCl	97.3
Slag 10 min H_2SO_4	97.6
Slag 15 min H_2SO_4	82.1
Slag plasma 10 min	100.0
Metal plasma 10 min	64.4

Table 7 : Chemical Composition of BR from Zvornik

Percent (%)	**Fe_2O_3**	**Al_2O_3**	**CaO**	**SiO_2**	**TiO_2**	**Na_2O**	**Cr_2O_3**	**Sc (ppm)**
Zvornik	49.3	12.0	8.2	10.5	4.6	2.5	0.13	76

This table 7 above shows that the bauxite residue from Zvornik, Bosnia and Hercegovina contains mostly Iron oxide. Bauxite residue was provided from Alumina D.O, Zvornik, Bosnia and Herzegowina, as the starting raw material. The factory Alumina has been in continuous production mode since October 6, 1978 and continuously processes bauxite and produces alumina, hydrates, zeolites and other related aluminosilicate products. The company Alumina currently has about 1500 employees, which is about 25% of all employees in Zvornik. Alumina owns a red mud disposal site located about 5 km from the factory. Transportation of the red mud suspension from the factory to the landfill is carried out by suitable pumps. The area of the red sludge landfill is about 1 km^2, as shown at Figure 18.

Figure 18:The area of accumulated Bauxite residue in Zvornik, Bosnia and Hercegowina.

During the operation of the company Alumina doo, about 19.4 x 106 m^3 of red mud suspension was disposed of. Depending on the quality of the bauxite, the amount of completely dry red mud typically ranges from 0.8 to 2 tons of tailings per ton of alumina produced. The company Alumina doo from Zvornik uses bauxite with a silicon dioxide modulus between 8.5 and 12. Accordingly, the amount of red mud that is separated and disposed of at the landfill is about 1.0 - 1.2 tons per ton of Al_2O_3 produced, or approximately 400,000 t / per year. The installed technical-technological equipment at the clearing plant is of a continuous (uninterrupted) nature, where there are five installed autoclave batteries of 11-12 interconnected autoclaves in series (each autoclave has 50 m^3). The bauxite residue from Alumina was filtrated, washed and dried at 105 °C for 24 h. The chemical composition of bauxite residue is shown in Table 9. Some compounds happen to exist in a little or no content in terms of percentage , and some have a larger chemical composition percentage. Fe_2O_3 has the highest percentage that is like 49.29%, followed by Al_2O_3, SiO_3, CaO, TiO, Na_2O e.t.c have a percentage range between 1-13% and all other compounds have percentages less than 1.

Table 8: Chemical Composition of Red Mud

Compounds	%	Compounds	%
Ignition loss at 1000°C	8,32	**Ga_2O_3**	0,225
SiO_2	10,52	**CuO**	0,007
Fe_2O_3	49,29	**K_2O**	0,159
Na_2O	2,45	**Tl_2O_3**	0,088
TiO_2	4,59	**MnO**	0,145
CaO	8,23	**MgO**	0,627
Al_2O_3	12,03	**NiO**	0,034
Ag_2O	0,001	**PbO**	0,019
BaO	0,014	**P_2O_5**	0,930
Cr_2O_3	0,133	**ZnO**	0,016
Sc_2O_3	0,011	**V_2O_5**	0,135
Co_2O_3	0,012	**SrO**	0,075

An additional elemental ICP -OES analysis was performed in order to establish the chemical composition presented in BR, Zvornik, see this in Table 9. The composition of the other elements in the bauxite residue used for this work is shown in Table 10, showing Celsium to be present in abundance.

Table 9 : Content of rare earth elements in BR, Zvornik

Content	Pr	**Sc**	**Y**	**La**	**Ce**	**Nd**	**Sm**	**Tb**	**total**
ppm	12	76	133	114	250	96	11	8	700

XRD-analysis found the following phases: hematite, perovskite, cancrinite, cancrinite, Ilmenite, calcite, diaspore, gibbsite and hydrogarnet. Iron is available in hematite and ilmenite structure. Titanium is present in Perovskite and ilmenite structure, while aluminum is available structure of in cancrinite, diaspore, boehmite, gibbsite and hydrogarnet, clearly seen in the figure 19 and table 11 below.

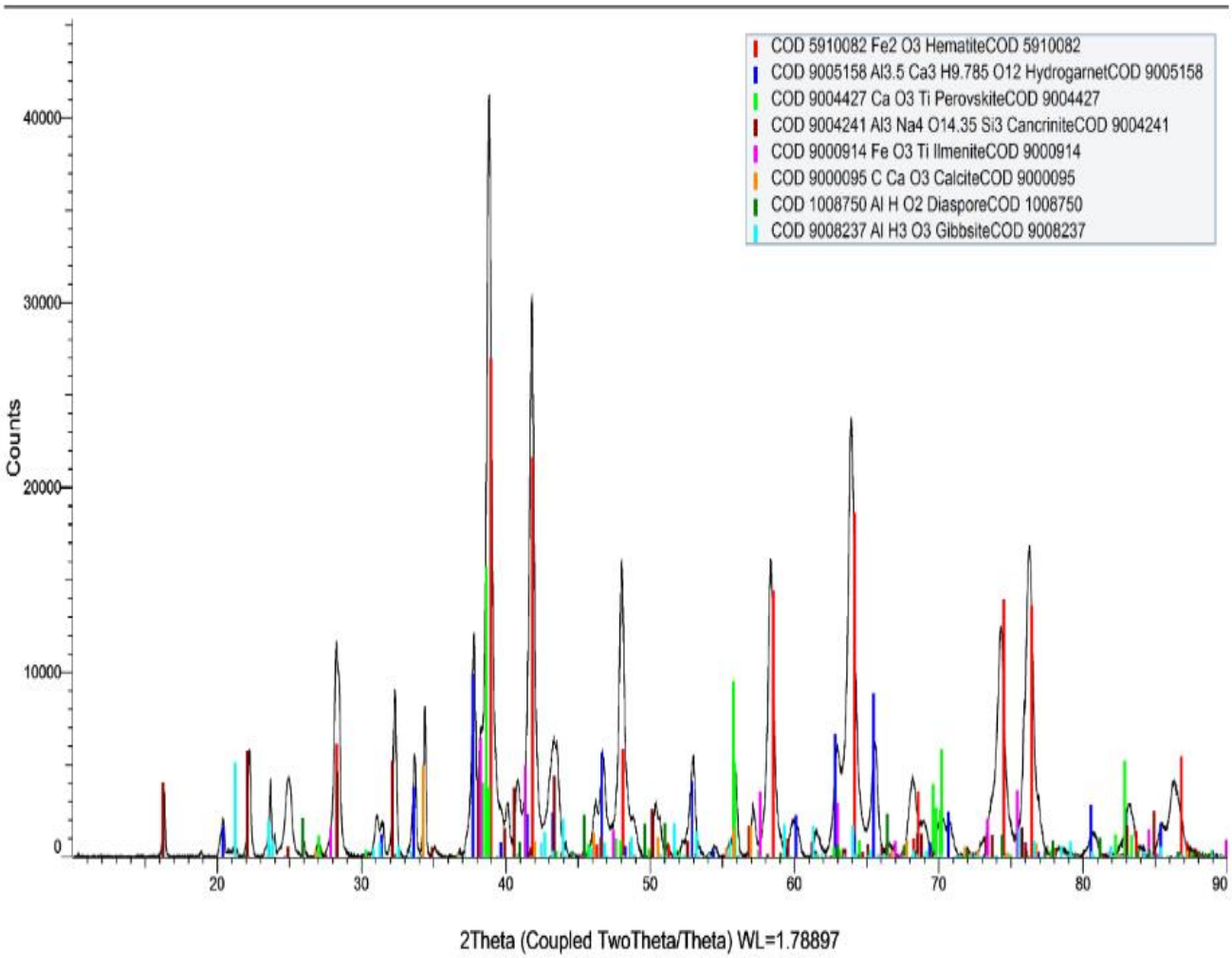

Figure 19 : XRD-analysis of BR from Zvornik

Table 10**:** X-ray diffraction analysis of red mud

METALS	MINERALS
Fe2O3	Hematite
Al3O, Ca3H9.785O12	Hydrogarnet
CaO3, Ti	Perovskite
Al3Na+O14.35 Si3	Cancrinite
Fe3O, Ti	ilmenite
C, CaO3	Calcite
AJ, HO2	Diaspore
AJ, H3O3	Gibbsite

3.2.HYDROMETALLURGICAL METHOD RESULTS

The first experiments were performed in order to study change of mineralogical structure during leaching experiment. The leaching was performed using the 1mol/l hydrochloric acid and 1mol/L sulfuric acid at 90 °C with solid/liquid ratio 1:10 and mixing rate 200 rpm for 120 mins (2hrs). The obtained XRD-Analysis were shown in Figures 20, 21, 22, and 23 respectively.

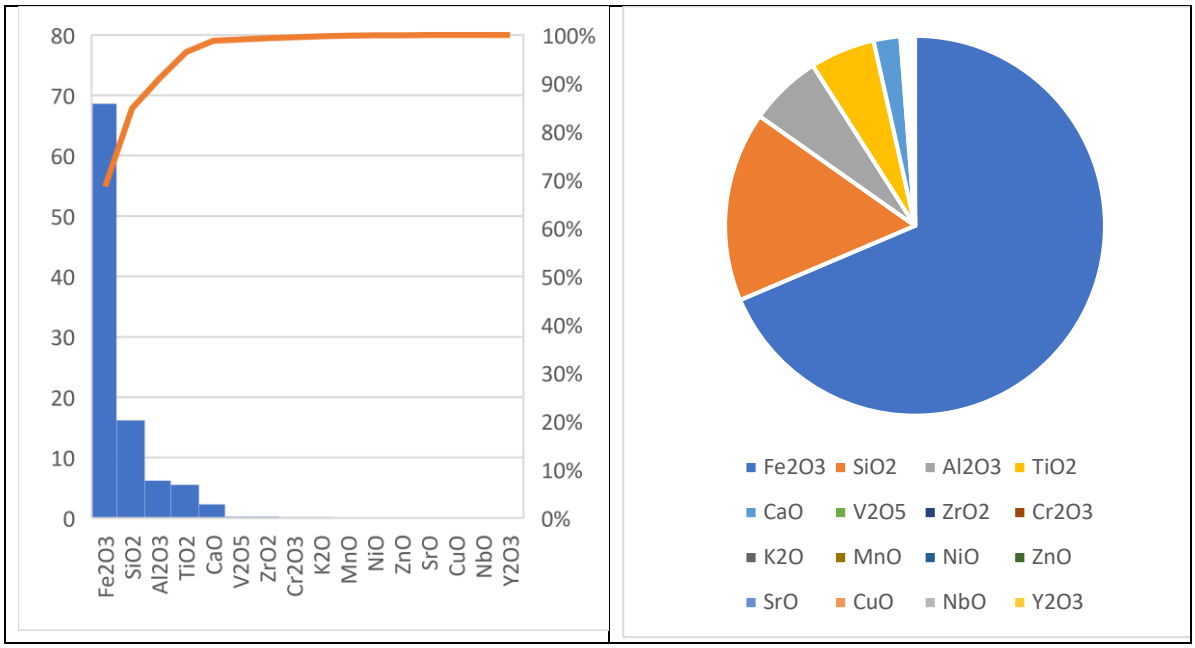

Figure 20 : Redmud (15.05.2023) with 1 mol/L HCl, 90 °C, 120 min (Graphical representation)

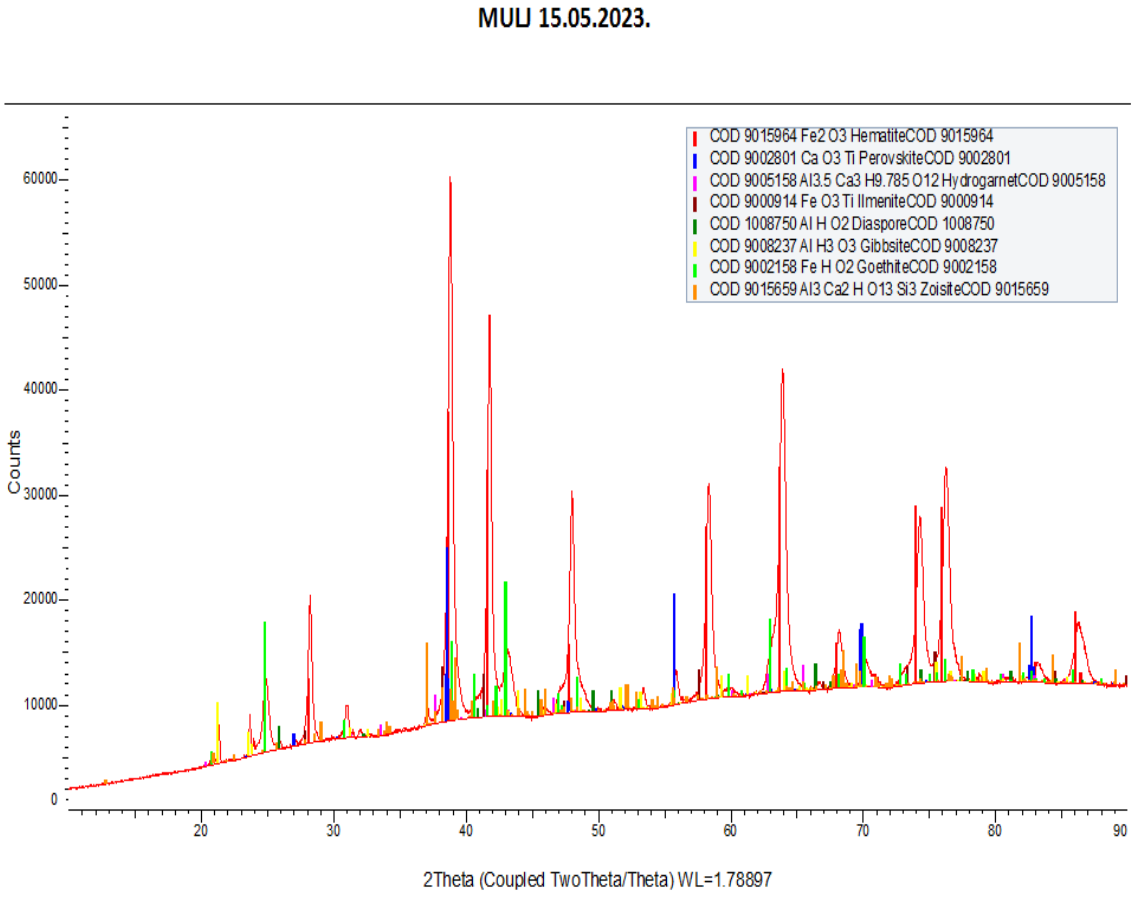

Figure 21 : Redmud with 1 mol/L HCl, 90 °C, 120 min

Redmud, was leached using 1 mol/L HCl, 90 °C, 120 min, Composition Hematite(Fe_2O_3,),Perovskite($CaTiO_3$),Hydrogarnet($Al_{3.5}Ca_3H_{9.875}O_{12}$), Diaspore(AlOOH), Gibbsite($Al(OH)_3$), Goethite(FeOOH), Zoisite($Ca_2Al_3(SiO_4)(Si_2O_7)O(OH)$) and Leaching of red mud without reduction confirms that the mineral structure is not changed.

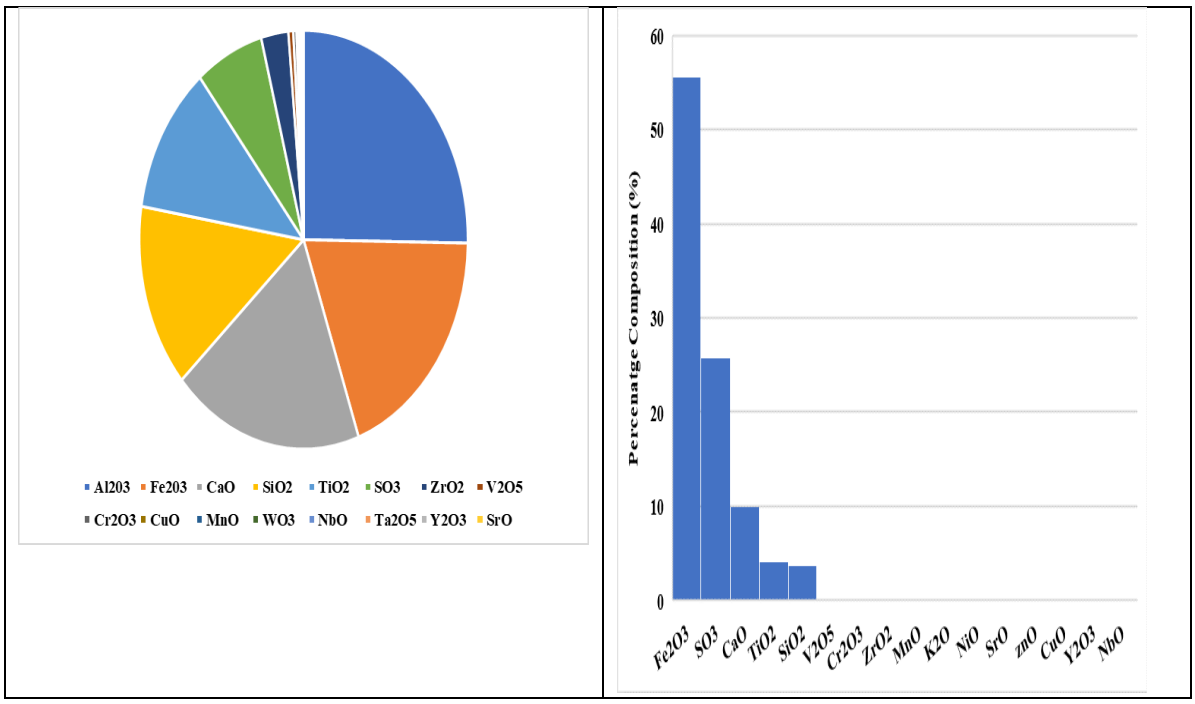

Figure 22: Redmud 17.05,2023 with 1 mol/L H_2SO_4,90°C, 120 min (Graphical representation)

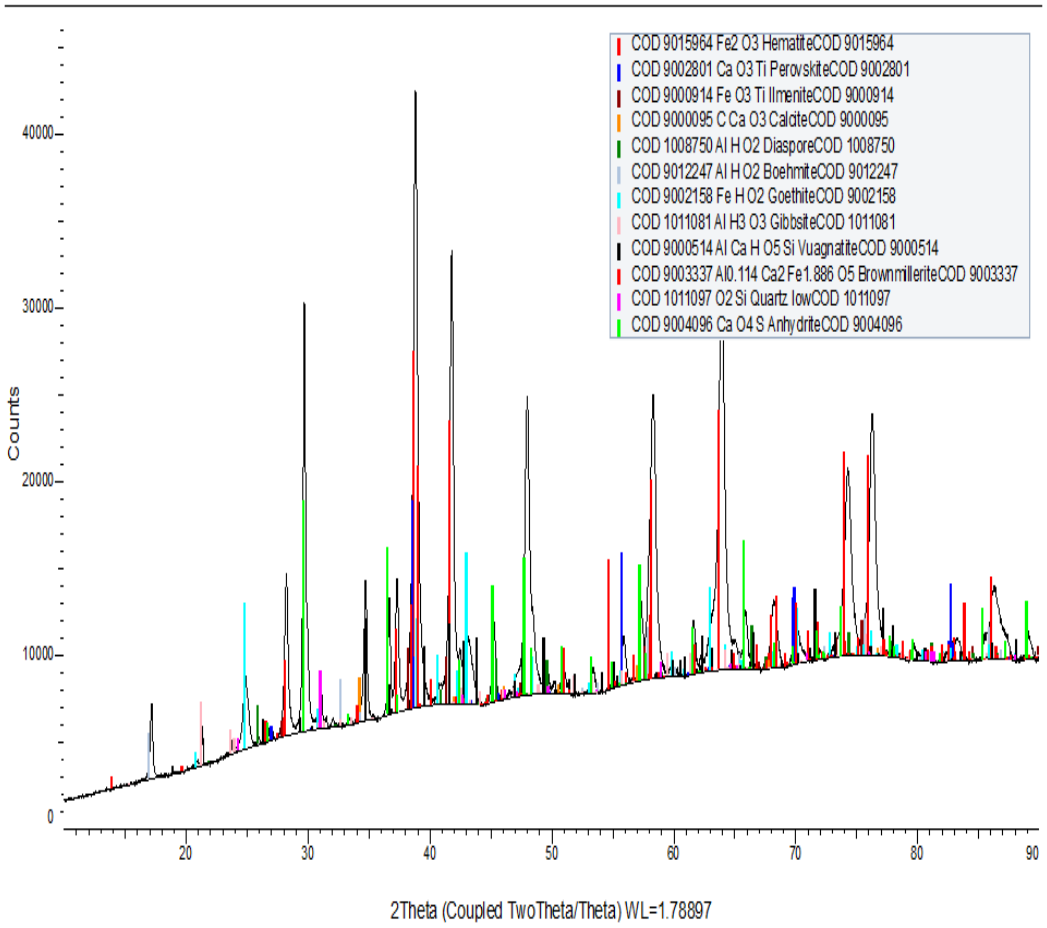

Figure 23 Redmud 17.05,2023 with 1 mol/L H_2SO_4,90 °C, 120 min

The results confirmed that Al_2O_3 and TiO_2 can not be reduced in Hydrogen Plasma Reduction Process but only Iron oxide (Fe_2O_3) was reduced as shown in figure 24.

Material(Redmud 17.05.2023), Process (Leaching of redmud using 1 mol/L H_2SO_4, 90 °C, 120 min), Composition (Hematite, Perovskite, Ilmenite, Calcite, Diaspore, Boehmite, Goethite, Gibsite, Vuagnatit, Brownmillerite, Quartz, Anhydrite). Mineralogical composition (Fe_2O_3, $CaTiO_3$, $FeTiO_3$, $CaCO_3$, α-AlOOH, Y-AlOOH, FeOOH, $Al(OH)_3$, $CaAlSiO_4(OH)$, $Ca_2(Al,Fe)_2O_5$, SiO_2, $CaSO_4$. Leaching of red mud without reduction confirms that the mineral structure is not only changed, but also some new comounds are Formed (Vuagnitit, Brownmillerite, Anhydrite).

Table 11: Comparative analysis of mineralogical phases of red mud after leaching

Material	Process	Mineral	Phase composition
Red mud (Bauxite residue)	Bayer (autoclave) T=150°C t=2 hours addition of NaOH	Hematite Perovskite Cancrinite Ilmenite Calcite Diaspore Gibbsite Hydrogarnet	Fe_2O_3 $CaTiO_3$ $Al_3Si_3Na_4O_{14.35}$ $FeTiO_3$ $CaCO_3$ AlOOH $Al(OH)_3$ $Al_{3.5}Ca_3H_{9.875}O_{12}$
Solid residue after a leaching of BR with hydrochloric acid	Leaching of BR using 1 mol/L HCl, 90 °C, 120 min	Hematite Perovskite Hydrogarnet Diaspore Gibbsite Goethite Zoisite	Fe_2O_3 $CaTiO_3$ $Al_{3.5}Ca_3H_{9.875}O_{12}$ AlOOH $Al(OH)_3$ FeOOH $Ca_2Al_3(SiO_4)(Si_2O_7)O(OH)$
Solid residue after a leaching of BR with sulfuric acid	Leaching of BR using 1 mol/L H_2SO_4, 90 °C, 120 min	Hematite Perovskite Ilmenite Calcite Diaspore Boehmite Goethite Gibsite Vuagnatit Brownmillerite Quartz Anhydrite	Fe_2O_3 $CaTiO_3$ $FeTiO_3$ $CaCO_3$ α-AlOOH Y-AlOOH FeOOH $Al(OH)_3$ $CaAlSiO_4(OH)$ $Ca_2(Al,Fe)_2O_5$ SiO_2 $CaSO_4$

The comparative analysis of the obtained XRD-analysis is presented in Table 12. Analysis of initial bauxite residue at Figure 23 has shown that Fe is present in hematite and ilmenite structure, Ti in Perovskite and ilmenite and Al in cancrinite, diaspore, boehmite, gibbsite and hydrogarnet. Leaching of BR without reduction confirms that the mineral structure was not changed, as shown at table 12. Direct Leaching of BR (as shown at Figure 20, 21, 22 and 23) confirms that the mineral structure is not only changed, but also some new compounds are found such as vuagnitit, brownmillerite, anhydrite, as shown at Figure 21, and 23. An addition of sulphuric acid leads to

formation of unsoluble calcium sulphate. The view of the results represent an unfavourable material to recover-earths by acid leaching, due to the high content of silicon, aluminium and iron. It must be noted that during the acid leaching with different temperatures an over-saturation of silica in acid solution can lead to silica polymerization due to the hydrolysis of the silica monomers, i.e. H_4SiO_4 and H_3SiO_4 -, formed during the decomposition of silicate compounds, the similar result were gotten by (Hamouda & Amiri, 2014), (Tobler et al., 2009), and (Kokhanenko et al., 2016) during their work related to this.

Table 12: Chemical composition of the obtained solution and calculated leaching efficiency

Elementsfrom solutions are presented as compounds	**Leaching with 1M HCl (90°C, 2hours, s/L: 1/10)**		**Leaching with 1M H_2SO_4 (90°C, 2hours, s/L: 1/10)**	
	Content (mg/L)	Leaching Efficiency (%)	Content (mg/L)	Leaching Efficiency (%)
Al_2O_3	7190	59.76	7292	60.61
SiO_2	2351	22.34	1369	13.01
P_2O_5	84.7	9.10	128.1	13.76
V_2O_5	8.8	6.51	41.4	30.66
SrO	12.6	16.8	7.9	10.53
Ga_2O_3	10,9	4.84	22.4	9.95
K_2O	46.2	29.05	56.4	35.47
Y_2O_3	16.3	9.65	13.6	8.05
NiO	4.44	13.08	9.1	26.76
Cr_2O_3	15.3	11.50	19.1	14.36
MnO	11.2	7.7	15.2	10.45
Ce_2O_3	13.3	4.54	4.0	1.37
Sc_2O_3	4.98	45.27	5.82	52.90
PbO	5.27	27.73	4.4	23.16
Fe_2O_3	718	1.46	1096	2.23
TiO_2	233	5.07	441	9.60

The maximal leaching efficiency was for aluminum for both chosen acids, is about 60 %. The small leaching efficiency has confirmed that the leaching time from 2 hours was not enough to ensure complete leaching efficiency. Leaching efficiency from scandium is maximal for rare earth elements, but not sufficient. Therefore, the increased concentration of solution, reaction temperature, and duration of process will be considered in order to

increase leaching efficiency.

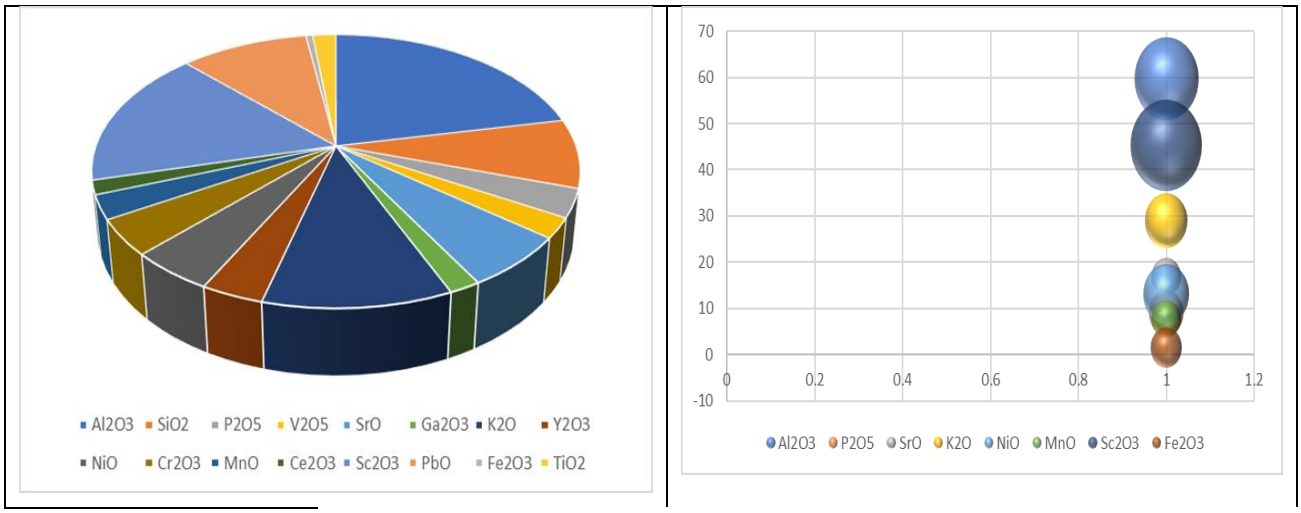

Figure 24 : Compounds (X-axis)- leaching Efficiency (Y-axis) Leaching with 1M HCl (90°C, 2hours, s/L: 1/10)

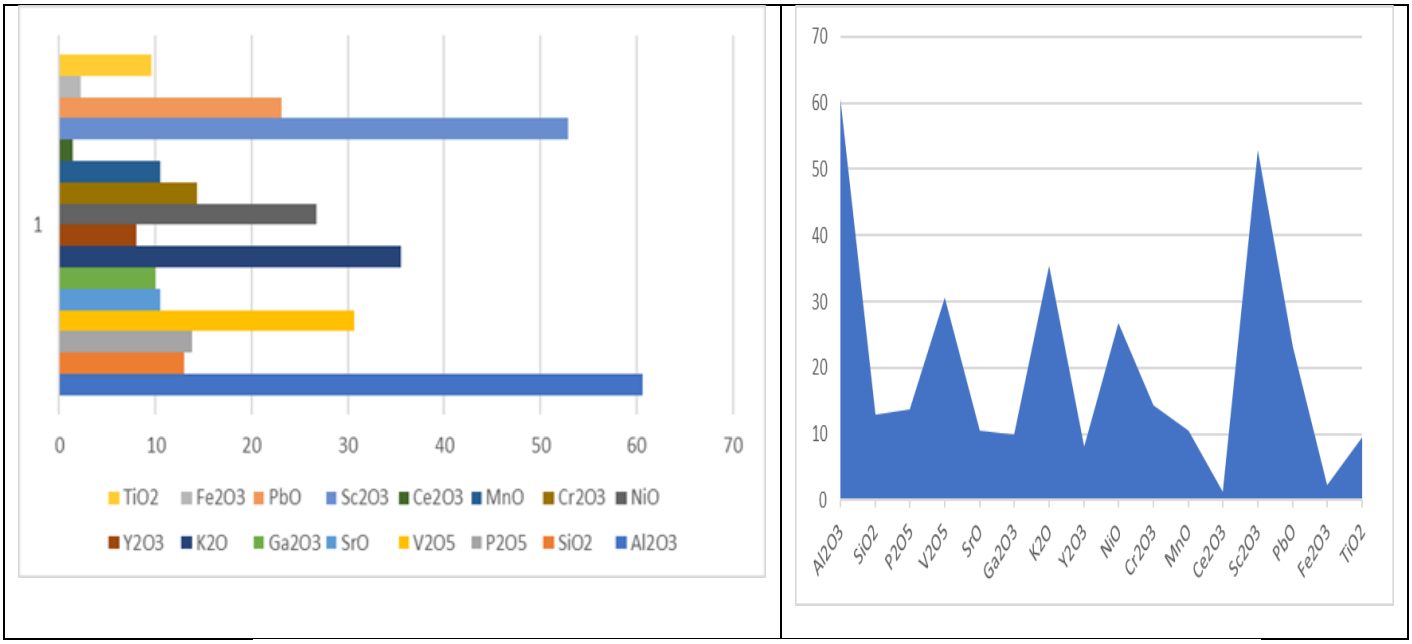

Figure 25 : Compounds (X-axis)- leaching Efficiency (Y-axis) Leaching with 1M H2SO4 (90°C, 2hours, s/L: 1/10)

Figure 26*:Formation of silica gel after sulfuric acid leaching at 90°C*

Using leaching process under an atmospheric pressure a formation of silica gel is confirmed for using a sulfuric acid as shown in Figure 26. Natural precipitation of iron form the obtained solution has confirmed after leaching with hydrochloric acid, as shown at Figure 27.

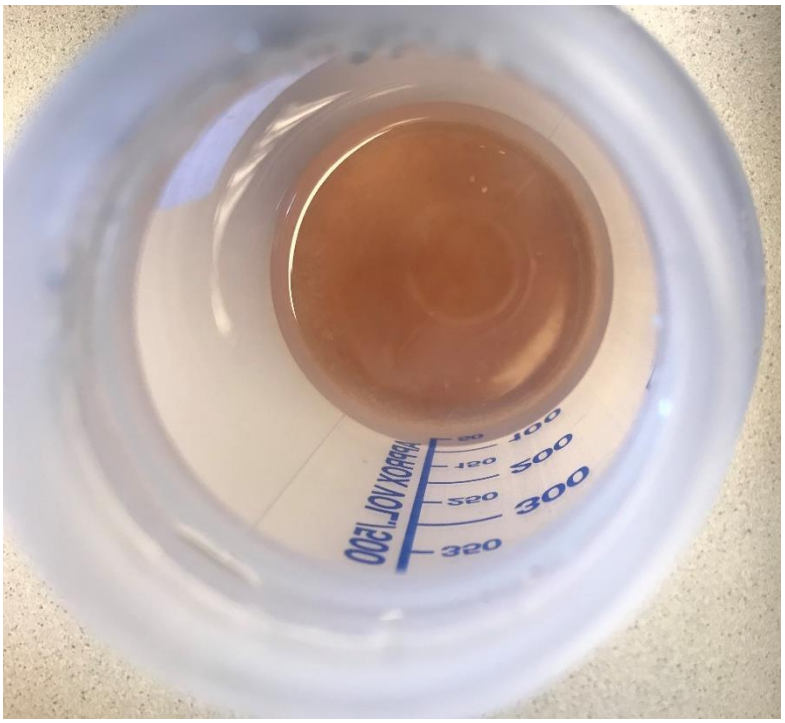

Figure 27: Natural precipitation of iron after hydrochloric acid leaching at 90°C

Formation of silica gel and natural precipitation of iron will be prevented through dry digestion process in the presence of hydrogen peroxide. The performed experiments of acidic leaching confirmed some difficulties relateted to direct leaching processs. Therefore, a high efficient technology shall be proposed to improve leaching efficiency of valuable metals. Pyrometallurgical method can ensure destroying mineralogical structure of bauxite residue forming more suitable slag structure for the better leaching using

different acids. A combined pyrometallurgical and hydrometallurgical method for treatment of bauxite residue will be reported in future in order to improve hydrometallurgical treatment. (Hamouda & Amiri, 2014) , (Alkan et al., 2018), and (Kokhanenko et al., 2016) also confirm according their work silica gel formation represents a serious drawback in hydrometallurgy because the gel solutions can no longer be filtered.

3.3 PYROMETALLURGICAL METHOD RESULTS

The experiments were performed in order to know the mineralogical structure of reducing BR using the hydrogen plasma reduction. 20g BR was used in the Electric arc furnace with a total pressure of 900 bar, 200A current, about 10% H2 gas, a temperature of 2500°C and different time variation(5, 10, & 15 minutes respectively). After reduction process of BR from Zvornik comprises metallic phase and slag, the slag was also leached with acids for further chemical and mineralogical composition that it has. After reduction, the mass of slag, mass of Iron metal and total mass after reduction was recorded for each time as represented graphically in figures 28 and 29. The valuable metals are concentrated in Slag because of the small content of Tungsten (W) in red mud (smaller than 1%). The high presence of tungsten (W) in metallic phase is surprising but W comes from the Cu electrode that was used during the reduction process. It is common that the electrode releases some small parts to the melt.

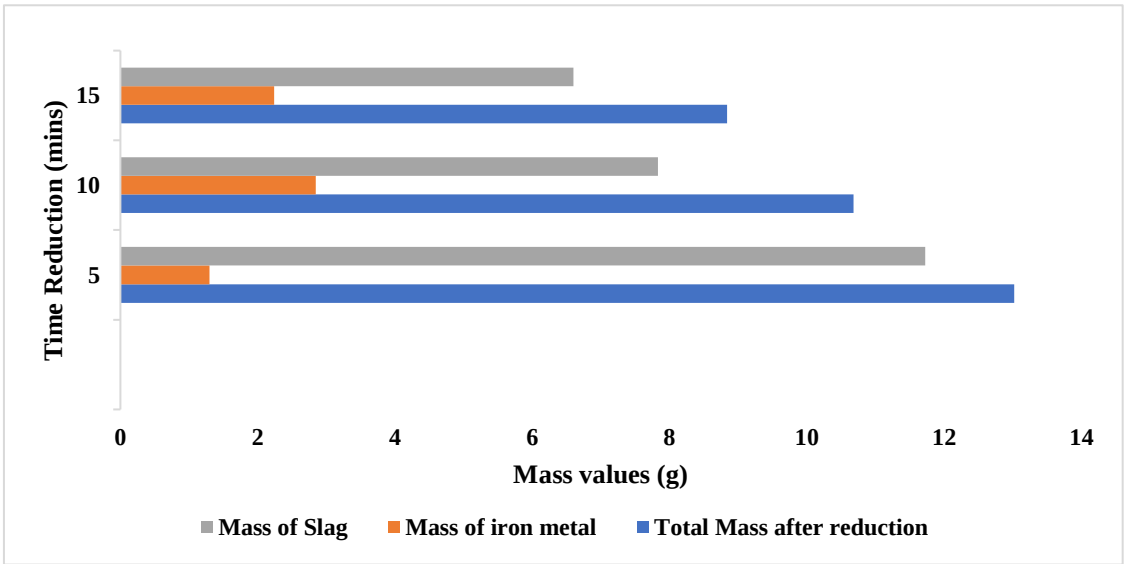

Figure 28 : Graphical representation of Reduction of red mud to slag(first set of 5, 10, and 15 Mins Experiments)

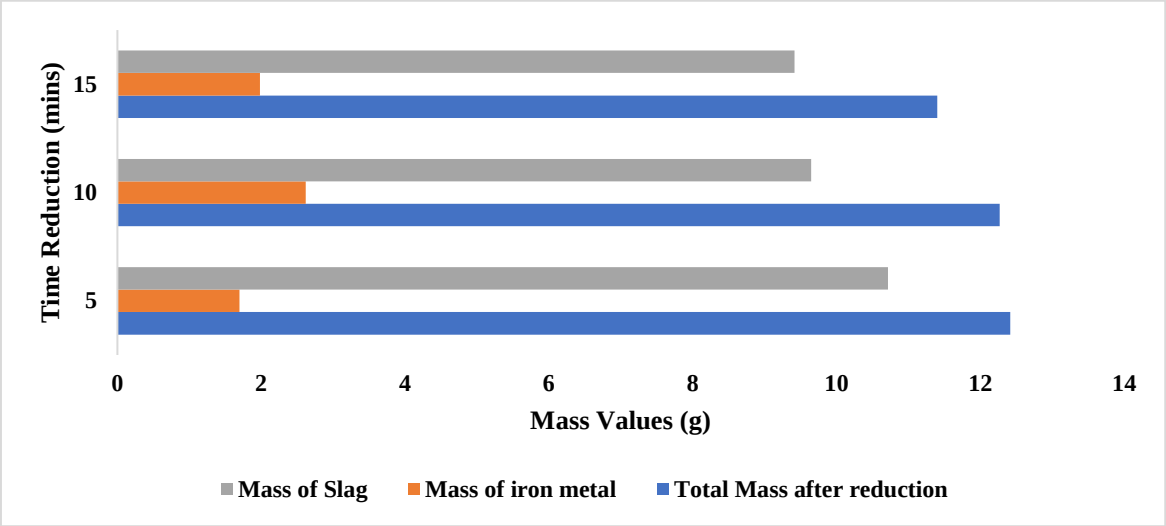

Figure 29 : Graphical representation of Reduction of red mud to slag(first set of 5, 10, and 15 Mins Experiments)

The results of chemical analysis of metallic phase after reduction in 10 mins. The results confirmed that Al_2O_3 and TiO_2 can not be reduced in Hydrogen Plasma Reduction Process but only Iron oxide (Fe_2O_3) was reduced as shown in the above figure. It was also necessary to grind the samples so that their granulation was about 50 µm, in order to make a pallet with a flat surface in polyethylene molds. With most of the samples, I could not fulfill this condition due to the hardness of the samples, which could not be crushed in an agate mortar. Despite the difficulties, I managed to create a pallet that did not have a flat surface, but I successfully performed the measurement. Only for the sample - " Metal plasma 10min", the measurement could not be performed.

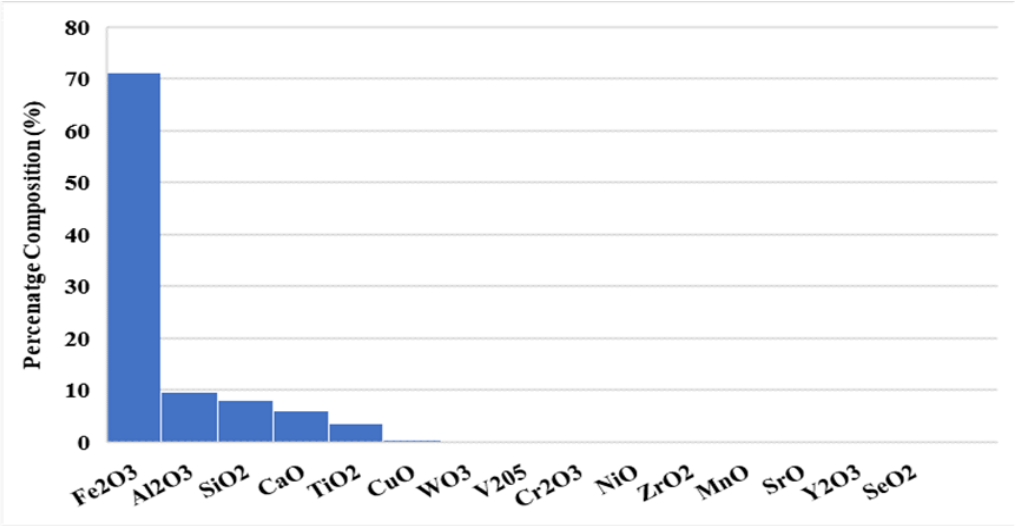

Figure 30 : Metallic Phase 10 Mins after Reduction

Al in Hercynite, Si in Fayalite, and Pyroxferroite, Cu in Cuprospinel and Ca in Pyroxferroite. Direct Leaching of slag (as shown in Figure 29 & 30) confirms that the mineral structure has not only changed, but also some new compounds are found when the acid was changed.

Table 13 : First set of hydrogen plasma reduction experience plus evaporates red mud

NO	Reduction Time (Mins)	Total Mass after Reduction (g)	Mass of Iron Metal (g)	Mass of Slag (g)	Mass of Evaporated Red Mud(g)
1	**5**	**13.02**	**1.300**	**11.725**	**6.98**
2	**10**	**10. 681**	**2.848**	**7.833**	**9.319**
3	**15**	**8.839**	**2.239**	**6.600**	**11.161**

Table 14 : Secomd set of hydrogen plasma reduction experience plus evaporates red mud

No	Reduction time (Mins)	Total Mass after Reduction (g)	Mass of Iron Metal (g)	Mass of Slag(g)	Mass of Evaporated Red Mud
1	**5**	**12.420**	**1.700**	**10.720**	**7.58**
2	**10**	**12.270**	**2.620**	**9.650**	**7.73**
3	**15**	**11.402**	**1.982**	**9.420**	**8.598**

Parameter for calculating the percentage of Slag, Metallic phase, and Evaporated red mud with an original mass of 20g red mud in the Arc Electric for reduction experiment.

Formular used is shown below:

Slag : 20 – (Metal + Evaporated red mud) / 20 x 100%

Metal : 20 – (Evaporated red mud + Slag) / 20 x 100%

Evaporated red mud : 20 – (Slag + Metal) / 20 x 100%

Fig. 31 shows the graphical representatins of the calculated percentage of metallic phase, slag, and evaporated red mud after reduction for different time intervals (5, 10, and 15 minutes) for the first batch. Tables 12 and 13 give a details description of the hydrogen plasma reduction process of the work, from using a 20g red mud in the arc furnace for each time interval, to calculating the mass of slas, metallic phase and evaporated material (red mud) into the atmosphere.

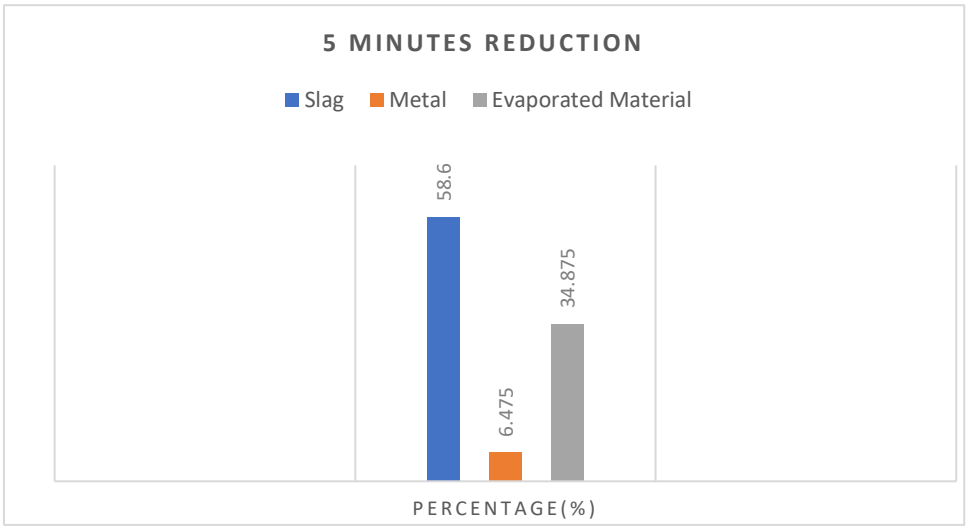

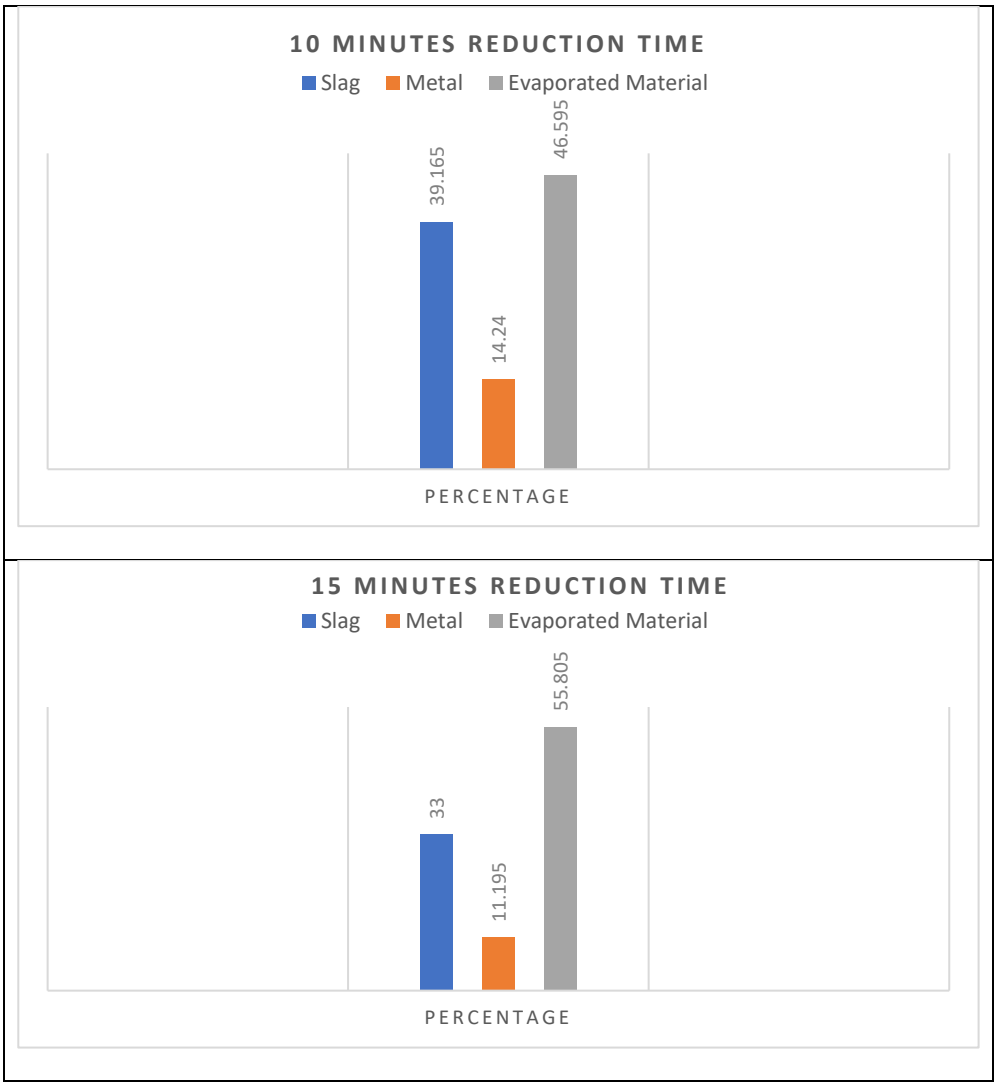

Figure 31 : Composition of Slag, Metallic Phase and Evaporated Material Present in Percentage

The XRD-Analysis of metallic phase has shown the presence of iron-alfa ferrite in figure 31. In other database we identified Fe and $FeNi_{0.16}$. (Valeev et al., 2020), (Spreitzer & Schenk, 2019), (Ma et al., 2022), and (Souza Filho et al., 2021). The presented XRD Analysis with Cu-CAthode, which is not enough suitable for the iron samples but the metallic phase will be analysed with Mo-cathode (XRD) and ICP OES analysis in order to improve the results. Figure 32 is a graphical representation of the iron ferrite diffraction present in one of the results during the metallic phase of my work.

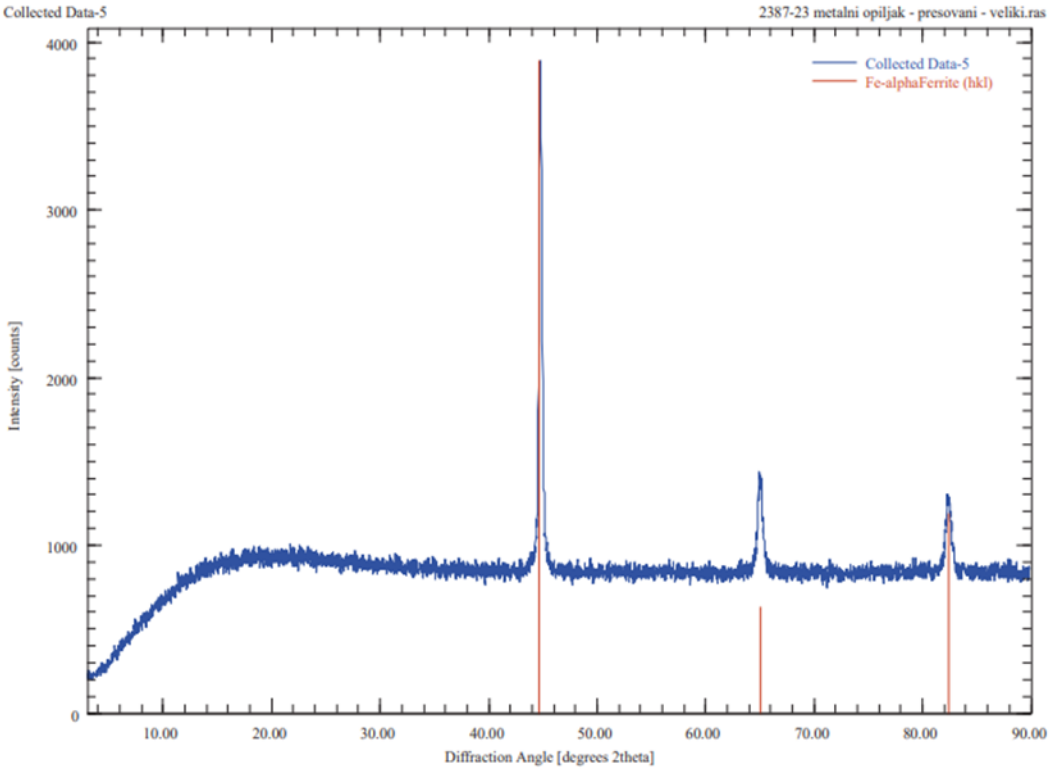

Figure 32 : XRD Analysis of Fe, and $FeNi_{0.16}$. of metallic phase

3.5 ICP OES ANALYSIS OF METALLIC PHASE

The results below in tables 16, and 17 shows the different elements that are found to be present in the experiment with their quantity.

Table 15 :First set of experiments for Metal (5 and 15 Minutes Reduction)

Sample number	Sample Designation	Al	Ce	Co	Fe	Ga	La	Nd	Pr
		%	ppm	ppm	ppm	ppm	ppm	ppm	ppm
I.0029.23.07.0349	Metal, 5min reduction	0,12 0,19	<50	163	Rest	90	<50	<50	<50
I.0029.23.07.0350	Metal, 15min reduction	0,27 0,58	<50	124	Rest	96	<50	<50	<50

Sample number	Sample Designation	Sc	Tb	Ti	V	Y
		ppm	ppm	ppm	ppm	ppm
I.0029.23.07.0349	Metal, 5min reduction	<50	<50	472 883	<50	<50
I.0029.23.07.0350	Metal,15min reduction	<50	<50	0,12% 0,24%	72 113	<50

Table 16 : Second Set of experiments for metals (5, 10, and 15 Minutes Reduction)

Sample Designation	Al	Ce	Co	Fe	Ga	La	Nd	Pr	W
	%	ppm	ppm	ppm	ppm	ppm	ppm	ppm	ppm
5 min	218 ppm	<50	254	98.8	89	<50	<50	<50	<50
10 min	0,220,075	<50	21787	Rest	106	<50	<50	<50	<50
15 min	0,40	<50	244154	Rest	112	<50	<50	<50	<50

Sample number	Sample Designation	Sc	Tb	Ti	V	Y
		ppm	ppm	ppm	ppm	ppm
I.0029.23.07.0251	5 min	<50	<50	68	<50	<50
I.0029.23.07.0252	10 min	<50	<50	954319	<50	<50
I.0029.23.07.0253	15 min	<50	ppm	0,18%	<50	<50

Table 18 shows the result of tungsten during the hydrogen plasma reduction experiment, tungsten was not initially part of the elements expected to be recovered in this but an of it was noticed to be found after the experiment when BR was reduced to slag and metallic phase.

Table 17 : Results for tungsten

Experiments	W
Bezeichnung	ppm
I.0029.23.06.0349-1 unverdünnt	-
I.0029.23.06.0349-2	-
I.0029.23.06.0350-1	5398,78
I.0029.23.06.0350-2	3341,54
I.0029.23.07.0251-1	-
I.0029.23.07.0251-2	-
I.0029.23.07.0252-1	4195,73
I.0029.23.07.0252-2	4466,96
I.0029.23.07.0253-1	2779,40
I.0029.23.07.0253-2	2475,53

3.4 LEACHING OF THE OBTAINED SLAG AFTER PLASMA REDUCTION

EDX analysis is an energy-dispersive X-ray technique with the help of which fluorescence is measured, thus quantifying the elements in the sample. For the analysis of the macrocomponents of the treated slag, the semiquantitative method was used in air, due to the imperfection of this technique (weak detection of trace elements under the given conditions), the ICP technique was used to determine the microimpurities. Samples measured in their original form without additional preparation, in polyethylene molds for measurement without vacuum in air conditions using the EDX 8000P Shimadzu device.

Table 19. shows the percentage of macro components present in slag after leaching for the different reduction times and also without leaching in Metallic phase. The presence of Fe2O3 is shown to be in abundance in the metallic phase without leaching, followed by slag 10 mins without leaching as well. Other components like SiO2, Al2O3, and TiO2 are also present in small quantities with or without leaching process.

Table 18 EDX macro components of Slag after leaching

	HCl		**H2SO4**		**No leaching**	
%	**Slag 10 min**	**Slag 15 min**	**Slag 10 min**	**Slag 15 min**	**Slag 10 min**	**METAL 10 min**
Fe_2O_3	26.02	19,31	9.73	5.06	29.94	71,18
SiO_2	14.66	14,23	4.98	2.56	17.41	8,13
Al_2O_3	21.35	25,26	4.41	2.72	21.41	9.76
TiO2 _	11,21	11.56	4.81	2.25	9.70	3.62

The Energy dispersive X-ray Analysis of the different phases after the Hydrogen plasma reduction experiments. The metal oxides present in each phase and the quantity, Table 19 gave a description of each and the oxides it is composed of. It helped in quantifying the elements in the sample.The comparative analysis of mineralogical phases of slag after leaching shows that during direct acidic leaching(H2SO4) with slag Fe is present in the hercynite and hedenbergite structure, Ti in Perovskite and Anatase and Al in Hercynite, Boehmite, and Zoisite, and Si in hedenbergite and Zoisite while leaching of slag with

HCL confirms the presence of Fe in Hercynite, Cuprospinel, Wüstite, Magnetite, Fayalite, and Pyroxferroite. Similarly Table 20 give a comparative analysis of mineralogical phases of slag after leaching with the different parameters used during each experiment.
Figure 34 and 35 below are examples of the graphical representations of the tabulated results for two sets of experiments with different parameters.

Table 19 Comparative analysis of mineralogical phases of slag after leaching

Material	Process	Mineral	Phase Composition
Slag 10 Mins	**Leaching with 1 mol** H2SO4, **T=90**°C, , 120 Mins, 2.5g Slag	Anatase Perovskite Hercynite Boehmite Hedenbergite Zoisite	TiO_2 $CaTiO_3$ $FeAl_2O_4$ AlOOH $CaFeSi_2O_6$ $Ca_2Al_3(SiO_4)(Si_2O_7)O(OH)$
Slag 10 Mins	**Leaching with 1 mol HCL, T=90**°C, 120 Mins, 2.5g Slag	Hercynite Cuprospinel Wüstite Magnetite Fayalite Pyroxferroite	$FeAl_2O_4$ $CuFe_2O_4$ $Fe_{0.994}O$ Fe_3O_4 $Fe_{2.001}Si_{0.99}O_4$ $Ca_{0.94}Fe_{6.06}Si_7O_{11}$

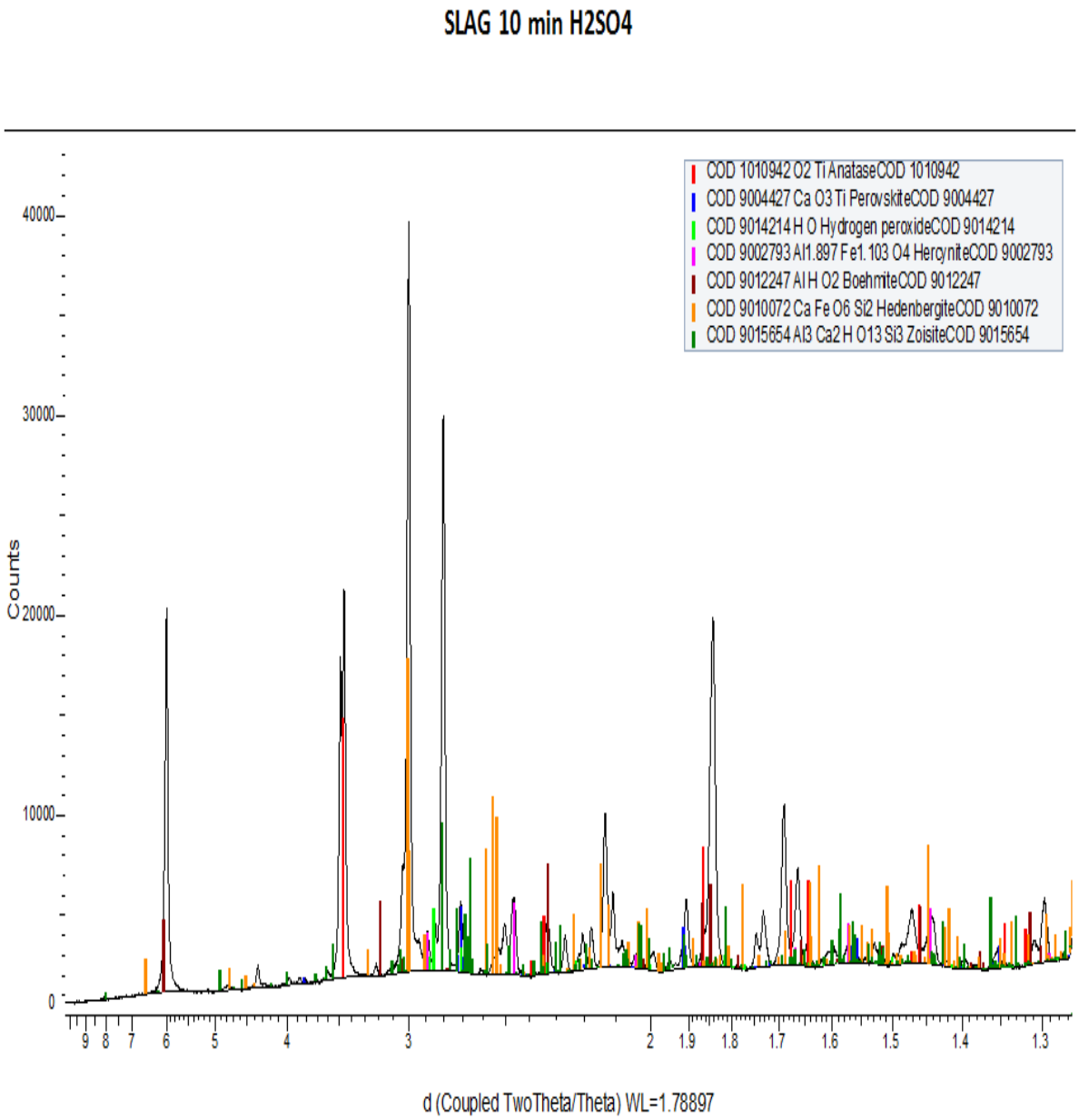

Figure 33 : Leaching 2.5g slag with 1 mol H2SO4, 90°C, 120mins

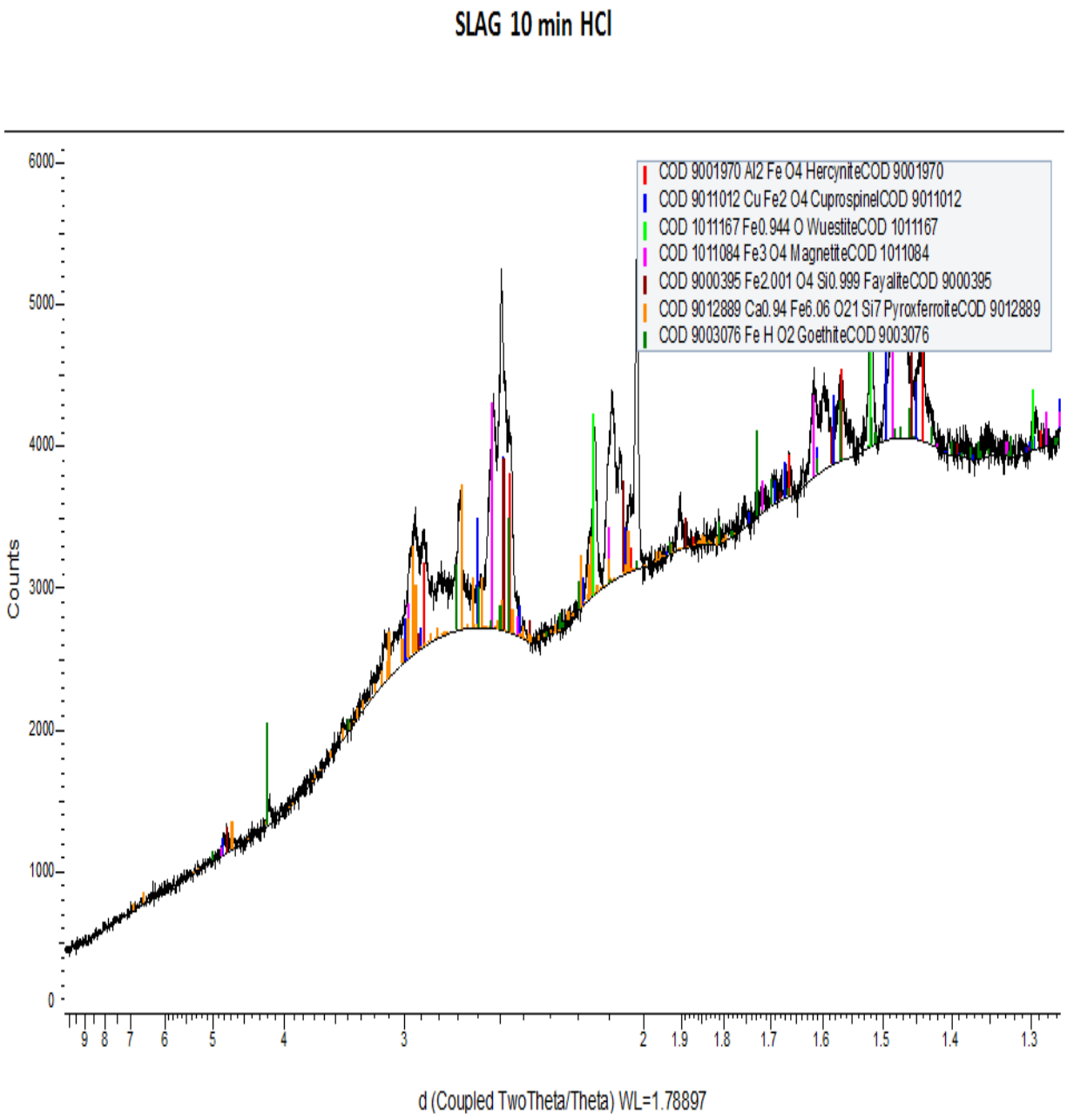

Figure 34 : Leaching 2.5g slag, with 1 mol HCL , 90°C, 120

3.5 Chemical Analysis Of Micro Impurities (ICP-OES Technique)

The elemental compositions of aqueous solutions were analyzed by either Inductively

Coupled Plasma – Optical Emission Spectrometry (ICP-OES) or Inductively Coupled Plasma – Mass Spectrometry (ICP-MS). The ICP-OES was used for the measurement of base metals (Fe, Al, Ca, Si, Na, K, Mg, Mn, Ti) and scandium for the bauxite residue experiments. The ICP- MS was used for the measurement of REEs, scandium, thorium, and uranium for the ionic clay experiments. For ICP-OES (PerkinElmer Optima 8000), the analysis was calibrated in the range of 0 to 20.0 mg/L for the measurement of (Fe, Al, Ca, Si, Na, K, Mg, Mn, Ti) in the radial viewing mode, and in the range of 0 to 0.05 mg/L for the measurement of scandium in the axial mode. Prior to measurement samples were diluted with 7.1 wt% HNO3 solution to ensure the analytes were within the calibration range. For ICP-MS (Thermo Scientific iCAP Q), the analysis was calibrated in the range of 0 to 200 μg/L. Prior to measurement, samples were diluted with 2.8 wt% HNO3 solution (for ICP-MS, high-purity ARISTAR® PLUS HNO3 was used) to ensure the analytes were within the calibration range. During analysis, 20 μg/L indium and bismuth solution was used as an internal standard.

In order to determine the micro impurities, we measured the samples on the ICP-OES device, an optical emission technique that uses inductively coupled plasma as a source. This technique is intended for the analysis of trace elements and requires the sample to be placed in an acidic solution.

Table 20 Results of micromixing (ICP-OES)

%	Leaching with HCl		Leaching with H2SO4		Initial slag	
	10 min	**15 min**	**10 min**	**15 min**	**slag 10 min**	**metal 15 min**
Ag_2O	0.0040	0.0047	0.0012	0.0011	0.0014	
BaO	0.033	0.034	0.039	0.034	0.034	0.010
CoO	0.010	0.012	0.009	0.008	0.011	0.008
Cr_2O_2	0.213	0.180	0.235	0.158	0.251	0.010
CuO	0.094	0.208	0.105	0.122	0.221	0.127
Ga_2O_3	0.576	0.576	0.484	0.399	0.330	0.051
In_2O_3	0.289	0.238	0.248	0.252	0.260	0.241
Li_2O	0.016	0.014	0.010	0.006	0.021	0.003
MgO	1,183	1,012	0.867	0.672	1,210	0.025
MnO	0.129	0.091	0.085	0.040	0.160	0.049
Na2O	0.49	0.91	0.12	0.06	2.07	
NiO	0.006	0.011	0.004	0.006	0.011	0.025
PbO	0.028	0.028	0.020	0.015	0.017	0.008
ZnO					0.003	

P_2O_5	5.84	12.01	5.90	6.74	10,13	6.49
V_2O_5	0.244	0.242	0.185	0.160	0.231	0.016
Sr.O	0.073	0.077	0.068	0.056	0.083	0.057
TlO_2	0.056	0.042				0.075
BiO_2	0.335	0.331	0.385	0.304	0.400	0.043
BeO	0.004	0.004	0.021	0.002	0.004	
Sc_2O_3	0.026	0.023	0.016	0.015	0.028	
Y_2O_3	0.040	0.041	0.026	0.028	0.030	
ZrO_2	1,393	1,499	0.224	0.196	0.251	0.009
MoO_2	0.001	0.001	0.003	0.000	0.004	0.002
Ce_2O_3	0.062	0.061	0.053			

Table 21 above shows the elemental composition of aqueous solutions were analyzed by the Inductively Coupled plasma- Optical Emission Spectrometry. The results in table 21 vary by different parameters, time, temperature etc. It also show different oxides found in the original material i.e Red mud use for the whole work. It shows the percentage of metals plus oxides present suring the different phases considered in the recovery. Equally Tabke 22 shows the leaching efficiency of slag with all the metal oxides present in the solid residue after leaching it with H_2SO_4 and HCL.

Table 21 : Leaching efficiency using values of content of oxides in slag and in solid residue after leaching of slag

%	**Calculation of leaching efficiency using values of content of oxides in slag and in solid residue after leaching of slag**			
	Slag (Reduction 10min)	**HCl-Leaching 90°C, 2h (leaching efficiency (%))**	**Slag (Reduction 10min)**	**H2SO4-Leaching 90°C, 2 h (leaching efficiency (%))**
Ag_2O	0,0014	0,0040 (formation of AgCl)	0,0014	0,0012 (14.28)
BaO	0,034	0,033 (2.94)	0,034	0,039 (formation of $BaSO_4$)
CoO	0,011	0,010 (9.09)	0,011	0,009 (18.18)
Cr_2O_3	0,251	0,213 (15.14)	0,251	0,235 (6.37)
CuO	0,221	0,094 (57.47)	0,221	0,105 (52.49)
Ga_2O_3	0,330	0,576 (formation of solid product)	0,330	0,484 (formation of some solid)
In_2O_3	0,260	0,289 (formation of solid product)	0,260	0,248 (4.61)
Li_2O	0,021	0,016 (23.81)	0,021	0,010 (52.38)
MgO	1,210	1,183 (23.23)	1,210	0,867 (28.34)
MnO	0,160	0,129 (19.38)	0,160	0,085 (46.88)
Na2O	2,07	0,49 (76.32)	2,07	0,12 (94.20)

NiO	0,011	0,006 (45.45)	0,011	0,004 (63.63)
PbO	0,017	0,028 (formation od solid product)	0,017	0,020 (formation of solid product)
P_2O_5	10,13	5,84 (42.34)	10,13	5,90 (41.75)
V_2O_5	0,231	0,244 (formation of solid product)	0,231	0,185 (19.91)
SrO	0,083	0,073 (12.05)	0,083	0,068 (18.07)
TlO_2	9.70	0.056 (99.36)	9.70	4.81 (50.41)
BiO_2	0,400	0,335 (16.25)	0,400	0,385 (3.75)
BeO	0,004	0,004 (no leaching)	0,004	0,021 (no leaching)
Sc_2O_3	0,028	0,026 (7.14)	0,028	0,016 (42.86)
Y_2O_3	0,030	0,040 (formation of solid)	0,030	0,026 (13.33)
ZrO_2	0,251	1,393 (formation of solid product)	0,251	0,224 (10.75)
MoO_2	0,004	0,001 (75.00)	0,001	0,001 (no leaching)
Ce_2O_3	0.077	0.062 (19.48)	0.077	0,061 (20.78)
SiO_2	17.41	14.66 (15.79)	17.41	4.98 (10.75)
Fe2O3	29.94	26.02 (13.09)	29.94	9.73 (67.5)
Al2O3	21.41	21.35 (0.28)	21.41	4.41 (79.40)
CaO	19.32	16.69 (13.61)	19.32	28.24 (formation of $CaSO_4$)

Shown below in figures 36 and 37 are the leaching efficiency results of Red Mud in a graphical representation. They show in percentage the mineralogical distribution of all the elements present in red mud after leaching it with either H_2SO_4 and HCL.

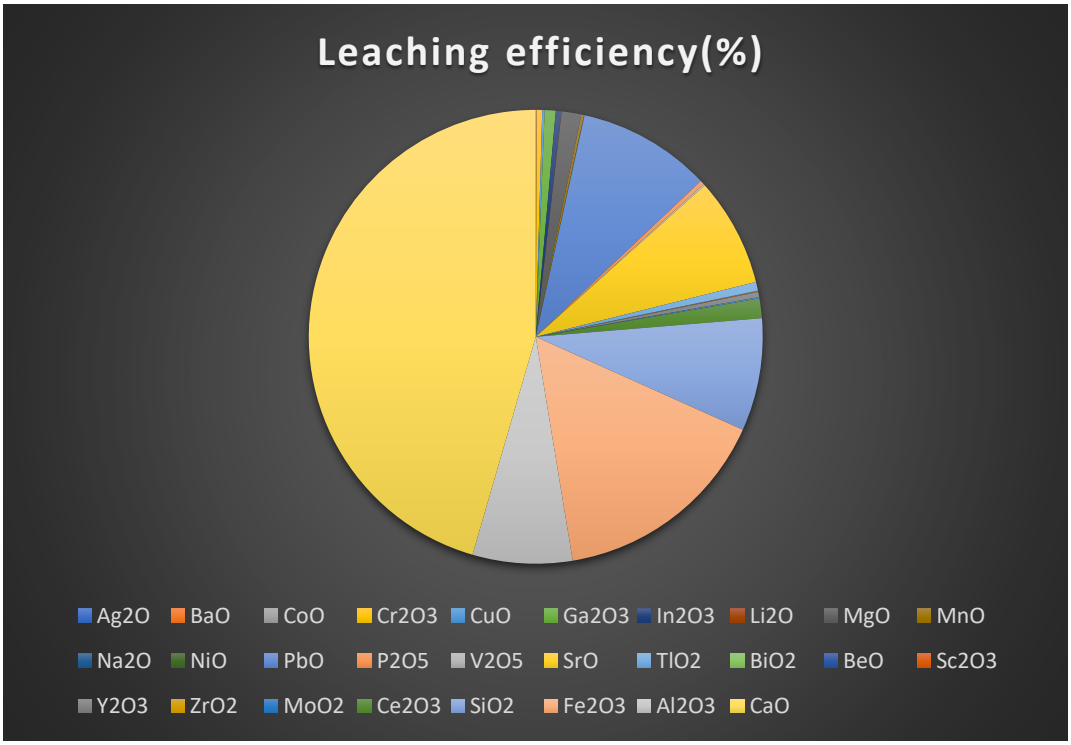

Figure 35 : HCl-Leaching 90°C, 2h (leaching efficiency (%))

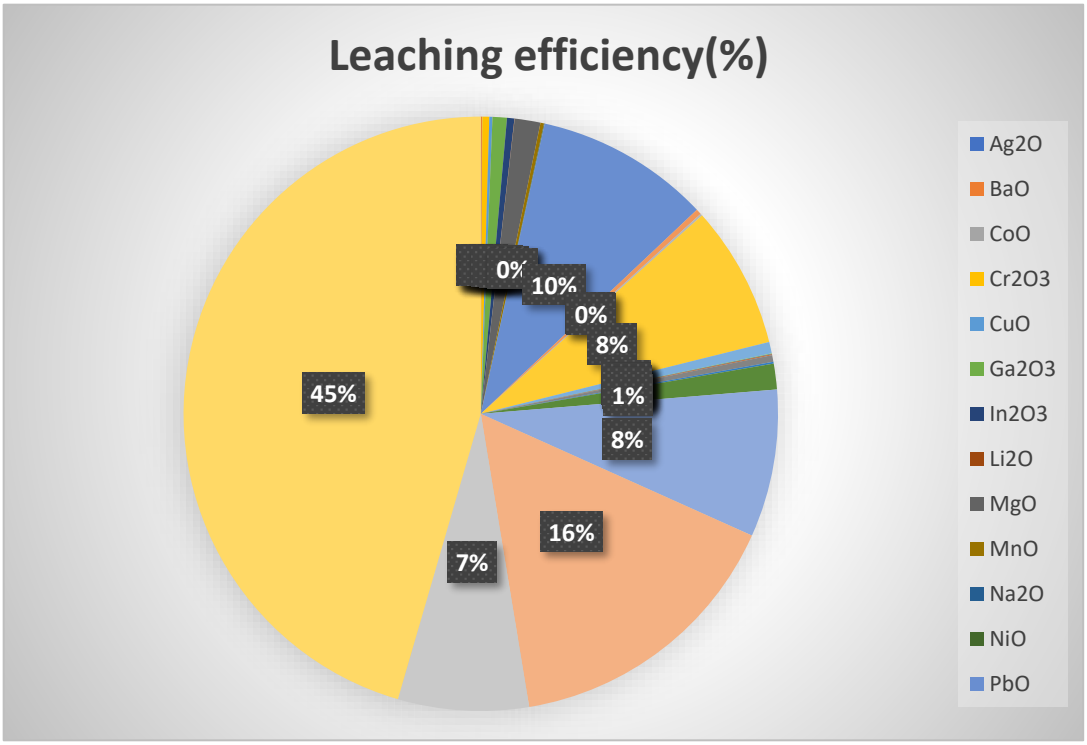

Figure 36 : H2SO4-Leaching 90°C, 2 h (leaching efficiency (%))

CONCLUSION AND RECOMMENDATION

CONCLUSION AND RECOMMENDATION

The recovery of valuable metals from bauxite residue was studied using pyrometallurgical and hydrometallurgical methods leading to new conclusions.

1. Decarbonized titanium recovery from bauxite redue from Alumina, Zvornik, Bosnia and Herzegovina is developed in this work. New research strategy contains hydrogen plasma reduction of red mud and subsequent leaching of the formed slag in order to recover from valuable metal such as titanium and rare earth elements. Metallic iron (99-99.5%) was separated from Slag and contains vey small amount of impurities
2. Hydrometallurgical treatment of bauxite residue with 1mol/lL hydrochloric acid and 1mol/L sulphuric acid at 90°C in 2hours leads to maximal leaching efficiency of about 60 % of aluminum, 50 % of scandium and minimal efficiency of other valuble elements, respectively. Formation of unsoluble calcium sulphate is present during leaching with sulphuric acid.
3. Analysis of changes in mineralogical structure during leaching of red mud has revaled that small changes are possible during hydrometallurgical treatment, showing, Hydrogarnet, Hematite, Pervskite, Diaspore, Gibbsite, Goethite, and Zoisite among others as the main minerals present during the direct acid leaching of bauxite residue from Zvornik, Bosnia and Hercegovina. This presence of these minerals proves the presence of Iron (49%) to be in abundance. Improved research strategy for treatment of bauxite residue is needed in order to ensure fully change an initial mineralogical structure and most efficient transfer of metals from bauxite rediues to liquid phase.
4. Pyrometallurgical treatment of BR using the hydrogen plasma reduction process shows the high extraction of metallic phase in 10 mins reduction time, about 71% efficiency of the metallic phase was attained, while efficient slag was attained in 5 mins reduction time. 39.16% Slag, 14.24% Metal and 46.60 % of evaporated material(BR) was achieved after 10 minutes hydrogen plasma reduction of BR in an electric arc furnace, what opens new possibilities for an application in industry. Therefore leaching of this slag was investigated usin hydrochloric and sulfuric acid.
5. Calcium sulphate was found in leaching of slag 10 minutes reduction time for 2 hours with both H2SO4 nad HCL, also a new compound Cuprospinel is present in

HCL leaching with slag 10 minutes reduction time for 2 hour. Anatase, Perovskite, Hercynite, Boehmite, Hedenbergite, Zoisite, Cuprospinel, Wüstite, Magnetite, Fayalite, and Pyroxferroite were the main minerals when leaching slag with acids. Fe, Al, Si etc. were present in abundance with new components that are observed.

Our recommendation are shown below:

- For future of hydrometallurgical treatment of BR, to achieve a high efficiency from the residue, hydrogen plasma reduction should be done before leaching with acids and hydrogen peroxide at higher temperatures in an autoclave and in ultrasound assisted leaching conditions in order to prevent the Silica gel formation and natural precipitation from iron from solution are some difficulties during my work.
- For future pyrometallurgical treatment of BR, the parameters (time, temperature and pressure) of the electric arc furnace should be optimised as per the objective of the work. The reduction time is the main determinate of the prcentage of evaporated material into the atmosphere, as the result clearly shows that, the higher the reduction time, the higher the evaporated material and the lower the time the lower the evaporated material as the case may be. This makes 10 mins reduction time a suitable time for future work if it aims at metallic phase extraction, 5 mins reduction time a suitabe time for slag extraction and 15 mins having a high evaporated material. This process shall be investigated in detail!

Bibliography

1. Alekseev, K., Mymrin, V., Avanci, M. A., Klitzke, W., Magalhães, W. L. E., Silva, P. R., Catai, R. E., Silva, D. A., & Ferraz, F. A. (2019). Environmentally clean construction materials from hazardous bauxite waste red mud and spent foundry sand. *Construction and Building Materials*, *229*. https://doi.org/10.1016/j.conbuildmat.2019.116860
2. Alkan, G., Yagmurlu, B., Cakmakoglu, S., Hertel, T., Kaya, Ş., Gronen, L., Stopic, S., & Friedrich, B. (2018). Novel Approach for Enhanced Scandium and Titanium Leaching Efficiency from Bauxite Residue with Suppressed Silica Gel Formation. *Scientific Reports*, *8*(1). https://doi.org/10.1038/s41598-018-24077-9
3. Anton, A. D., Klebercz, O., Magyar, A., Burke, I. T., Jarvis, A. P., Gruiz, K., & Mayes, W. M. (2014). Geochemical recovery of the Torna-Marcal river system after the Ajka red mud spill, Hungary. *Environmental Science: Processes and Impacts*, *16*(12), 2677–2685. https://doi.org/10.1039/c4em00452c
4. Archambo, M., & Kawatra, S. K. (2021). Red Mud: Fundamentals and New Avenues for Utilization. In *Mineral Processing and Extractive Metallurgy Review* (Vol. 42, Issue 7, pp. 427–450). Taylor and Francis Ltd. https://doi.org/10.1080/08827508.2020.1781109
5. Bədənoiu, A. I., Abood Al-Saadi, T. H., & Voicu, G. (2015). Synthesis and properties of new materials produced by alkaline activation of glass cullet and red mud. *International Journal of Mineral Processing*, *135*, 1–10. https://doi.org/10.1016/j.minpro.2014.12.002
6. Bogatyrev, B. A., Zhukov, V. V., & Tsekhovsky, Y. G. (2009). Formation conditions and regularities of the distribution of large and superlarge bauxite deposits. *Lithology and Mineral Resources*, *44*(2), 135–151. https://doi.org/10.1134/S0024490209020035
7. Borra, C. R., Pontikes, Y., Binnemans, K., & Van Gerven, T. (2015). Leaching of rare earths from bauxite residue (red mud). *Minerals Engineering*, *76*, 20–27. https://doi.org/10.1016/j.mineng.2015.01.005

8. Filho, S., Alves, E. B. ;, & Da Motta, M. C. M. ; (2007). Lama vermelha da indústria de beneficiamento de alumina: produção, características, disposição e aplicações alternativas Red mud: An environmental problem in alumina industry. *Revista Matéria*, *v*, *12*(2), 322–338. http://www.materia.coppe.ufrj.br/sarra/artigos/artigo10888
9. Gow, N. N., & Lozej, G. P. (1993). *Geoscience Canada Bauxite*. *20*(1).
10. Hairi, S. N. M., Jameson, G. N. L., Rogers, J. J., & MacKenzie, K. J. D. (2015). Synthesis and properties of inorganic polymers (geopolymers) derived from Bayer process residue (red mud) and bauxite. *Journal of Materials Science*, *50*(23), 7713–7724. https://doi.org/10.1007/s10853-015-9338-9
11. Hamouda, A. A., & Amiri, H. A. A. (2014). Factors affecting alkaline sodium silicate gelation for in-depth reservoir profile modification. *Energies*, *7*(2), 568–590. https://doi.org/10.3390/en7020568
12. Hu, Y., Liang, S., Yang, J., Chen, Y., Ye, N., Ke, Y., Tao, S., Xiao, K., Hu, J., Hou, H., Fan, W., Zhu, S., Zhang, Y., & Xiao, B. (2019). Role of Fe species in geopolymer synthesized from alkali-thermal pretreated Fe-rich Bayer red mud. *Construction and Building Materials*, *200*, 398–407. https://doi.org/10.1016/j.conbuildmat.2018.12.122
13. Ifg. (n.d.). *Construction of an unpaved road using industrial by-products (bauxite residue)*.
14. Khairul, M. A., Zanganeh, J., & Moghtaderi, B. (2019). The composition, recycling and utilisation of Bayer red mud. In *Resources, Conservation and Recycling* (Vol. 141, pp. 483–498). Elsevier B.V. https://doi.org/10.1016/j.resconrec.2018.11.006
15. Kokhanenko, P., Brown, K., & Jermy, M. (2016). Silica aquasols of incipient instability: Synthesis, growth kinetics and long term stability. *Colloids and Surfaces A: Physicochemical and Engineering Aspects*, *493*, 18–31. https://doi.org/10.1016/j.colsurfa.2015.10.026
16. Krivenko, P., Kovalchuk, O., Pasko, A., Croymans, T., Hult, M., Lutter, G., Vandevenne, N., Schreurs, S., & Schroeyers, W. (2017). Development of alkali activated cements and concrete mixture design with high volumes of

red mud. *Construction and Building Materials*, *151*, 819–826. https://doi.org/10.1016/j.conbuildmat.2017.06.031

17. Lemougna, P. N., Wang, K. tuo, Tang, Q., & Cui, X. min. (2017). Synthesis and characterization of low temperature (<800 °C) ceramics from red mud geopolymer precursor. *Construction and Building Materials*, *131*, 564–573. https://doi.org/10.1016/j.conbuildmat.2016.11.108
18. Lima, M. S. S., Thives, L. P., Haritonovs, V., & Bajars, K. (2017a). Red mud application in construction industry: Review of benefits and possibilities. *IOP Conference Series: Materials Science and Engineering*, *251*(1). https://doi.org/10.1088/1757-899X/251/1/012033
19. Lima, M. S. S., Thives, L. P., Haritonovs, V., & Bajars, K. (2017b). Red mud application in construction industry: Review of benefits and possibilities. *IOP Conference Series: Materials Science and Engineering*, *251*(1). https://doi.org/10.1088/1757-899X/251/1/012033
20. Lyu, F., Hu, Y., Wang, L., & Sun, W. (2021). Dealkalization processes of bauxite residue: A comprehensive review. In *Journal of Hazardous Materials* (Vol. 403). Elsevier B.V. https://doi.org/10.1016/j.jhazmat.2020.123671
21. Ma, Y., Souza Filho, I. R., Bai, Y., Schenk, J., Patisson, F., Beck, A., van Bokhoven, J. A., Willinger, M. G., Li, K., Xie, D., Ponge, D., Zaefferer, S., Gault, B., Mianroodi, J. R., & Raabe, D. (2022). Hierarchical nature of hydrogen-based direct reduction of iron oxides. *Scripta Materialia*, *213*. https://doi.org/10.1016/j.scriptamat.2022.114571
22. Manfroi, E. P., Cheriaf, M., & Rocha, J. C. (2014). Microstructure, mineralogy and environmental evaluation of cementitious composites produced with red mud waste. *Construction and Building Materials*, *67*, 29–36. https://doi.org/10.1016/j.conbuildmat.2013.10.031
23. Mercury, J. M. R., Cabral, A. A., Paiva, A. E. M., Angélica, R. S., Neves, R. F., & Scheller, T. (2011). Thermal behavior and evolution of the mineral phases of Brazilian red mud. *Journal of Thermal Analysis and Calorimetry*, *104*(2), 635–643. https://doi.org/10.1007/s10973-010-1039-7
24. Mukiza, E., Zhang, L. L., Liu, X., & Zhang, N. (2019). Utilization of red mud in road base and subgrade materials: A review. In *Resources*,

Conservation and Recycling (Vol. 141, pp. 187–199). Elsevier B.V. https://doi.org/10.1016/j.resconrec.2018.10.031

25. Power, G., Gräfe, M., & Klauber, C. (2011). Bauxite residue issues: I. Current management, disposal and storage practices. *Hydrometallurgy*, *108*(1–2), 33–45. https://doi.org/10.1016/J.HYDROMET.2011.02.006
26. Rai, S., Bahadure, S., Chaddha, M. J., & Agnihotri, A. (2020). Disposal Practices and Utilization of Red Mud (Bauxite Residue): A Review in Indian Context and Abroad. *Journal of Sustainable Metallurgy*, *6*(1), 1–8. https://doi.org/10.1007/s40831-019-00247-5
27. Ribeiro, D. V., Labrincha, J. A., & Morelli, M. R. (2011). Potential use of natural red mud as pozzolan for Portland cement. *Materials Research*, *14*(1), 60–66. https://doi.org/10.1590/S1516-14392011005000001
28. Ribeiro, D. V, Labrincha, J. A., & Morelli, M. R. (2012). Effect of red mud addition on the corrosion parameters of reinforced concrete evaluated by electrochemical methods. In *IBRACON Structures and Materials Journal • 2012 •* (Vol. 5, Issue 4).
29. Romano, R. C. de O., Bernardo, H. M., Maciel, M. H., Pileggi, R. G., & Cincotto, M. A. (2019). Using isothermal calorimetry, X-ray diffraction, thermogravimetry and FTIR to monitor the hydration reaction of Portland cements associated with red mud as a supplementary material. *Journal of Thermal Analysis and Calorimetry*, *137*(6), 1877–1890. https://doi.org/10.1007/s10973-019-08095-x
30. Shoppert, A. A., Loginova, I. V., Rogozhnikov, D. A., Karimov, K. A., & Chaikin, L. I. (2019). Increased As Adsorption on Maghemite-Containing Red Mud Prepared by the Alkali Fusion-Leaching Method. *Minerals*, *9*(1). https://doi.org/10.3390/min9010060
31. Silveira, N. C. G., Martins, M. L. F., Bezerra, A. C. S., & Araújo, F. G. S. (2021a). Red mud from the aluminium industry: Production, characteristics, and alternative applications in construction materials—a review. In *Sustainability (Switzerland)* (Vol. 13, Issue 22). MDPI. https://doi.org/10.3390/su132212741
32. Silveira, N. C. G., Martins, M. L. F., Bezerra, A. C. S., & Araújo, F. G. S. (2021b). Red mud from the aluminium industry: Production, characteristics,

and alternative applications in construction materials—a review. In *Sustainability (Switzerland)* (Vol. 13, Issue 22). MDPI. https://doi.org/10.3390/su132212741

33. Souza Filho, I. R., Ma, Y., Kulse, M., Ponge, D., Gault, B., Springer, H., & Raabe, D. (2021). Sustainable steel through hydrogen plasma reduction of iron ore: Process, kinetics, microstructure, chemistry. *Acta Materialia*, *213*. https://doi.org/10.1016/j.actamat.2021.116971
34. Spreitzer, D., & Schenk, J. (2019). Reduction of Iron Oxides with Hydrogen—A Review. In *Steel Research International* (Vol. 90, Issue 10). Wiley-VCH Verlag. https://doi.org/10.1002/srin.201900108
35. Stopić, S., & Friedrich, B. (2023). Formation and application of hydrogen in non-ferrous metallurgy. *Vojnotehnicki Glasnik*, *71*(3), 783–796. https://doi.org/10.5937/vojtehg71-43407
36. Tobler, D. J., Shaw, S., & Benning, L. G. (2009). Quantification of initial steps of nucleation and growth of silica nanoparticles: An in-situ SAXS and DLS study. *Geochimica et Cosmochimica Acta*, *73*(18), 5377–5393. https://doi.org/10.1016/j.gca.2009.06.002
37. Valeev, D., Zinoveev, D., Kondratiev, A., Lubyanoi, D., & Pankratov, D. (2020). Reductive smelting of neutralized red mud for iron recovery and produced pig iron for heat-resistant castings. *Metals*, *10*(1). https://doi.org/10.3390/met10010032
38. Verma, A. S., Suri, N. M., & Kant, S. (2017). Applications of bauxite residue: A mini-review. In *Waste Management and Research* (Vol. 35, Issue 10, pp. 999–1012). SAGE Publications Ltd. https://doi.org/10.1177/0734242X17720290
39. Wang, W., Pranolo, Y., & Cheng, C. Y. (2011). Metallurgical processes for scandium recovery from various resources: A review. *Hydrometallurgy*, *108*(1–2), 100–108. https://doi.org/10.1016/j.hydromet.2011.03.001
40. Zhang, Y., Xu, R., Tang, H., Wang, L., & Sun, W. (2020). A review on approaches for hazardous organics removal from Bayer liquors. In *Journal of Hazardous Materials* (Vol. 397). Elsevier B.V. https://doi.org/10.1016/j.jhazmat.2020.122772